International Journal of Solids and Structures 47 (2010) 1857–1870

Contents lists available at ScienceDirect

International Journal of Solids and Structures

journal homepage: www.elsevier.com/locate/ijsolstr

Eigenoscillations of three- and two-element flexible systems

I. Gavrilyuk [a], M. Hermann [b], Yu. Trotsenko [c], A. Timokha [d,*]

[a] Staatliche Studienakademie Thüringen Berufsakademie, Eisenach, Am Wartenberg 2, 99817 Eisenach, Germany
[b] Friedrich-Schiller-Universität Jena, Ernst-Abbe-Platz 2-4, Jena 07745, Germany
[c] Institute of Mathematics of NASU, Tereschenkivska, 3 Str., 01601 Kiev, Ukraine
[d] Centre for Ships and Ocean Structures, NTNU, NO-7491 Trondheim, Norway

ARTICLE INFO

Article history:
Received 26 October 2008
Received in revised form 16 March 2010
Available online 8 April 2010

Keywords:
Coupled beam–shell vibrations
Variational methods

ABSTRACT

Eigenfrequencies and eigenmodes of composite mechanical systems consisting of a thin-walled cylindrical shell and elastic beams [beam–shell–beam (BSB), beam–beam–beam (BBB), etc. systems] are described by using semi-analytical methods. The methods are less universal comparing with the Finite Element Method, but they are very accurate and CPU-efficient, and they could have advantages in studying multicomponent structures. A comparative analysis of eigenfrequencies and eigenmodes of the considered composite systems versus characteristic geometric dimensions is presented.

1. Introduction

Coupling long cylindrical rigid and elastic solids are common for aircraft, spacecraft, shipbuilding and other industry applications. An example is tall towers (see, Drake, 1999; Dutta et al., 2004; Livaoglu and Doganguen, 2006; Faltinsen and Timokha, 2009, and references cited therein). Another interesting example is related to carbon nanotubes (see Harik et al., 2002; Gibson et al., 2007, and references cited therein) with either a point mass (Wu et al., 2006) or another nanotube (Legoas et al., 2004; Gibson et al., 2007) attached to the nanotube end.

In these and other examples, the whole structure is rather complicated containing numerous rigid and elastic components and, moreover, may include fluid and gases interacting with these components and each other. Bearing in mind a simplification in modeling the coupled motions of the complex structure, one must decide which elementary components can be described by a rigid body, a beam, or a shell model. Because coupling the neighboring elementary components matters, a dedicated comparative study of shell–rigid body, shell–beam, beam–shell–beam, etc. systems as main macrocomponents of the whole structure is required. Eigenoscillations of these composite systems vary with the input geometric and physical parameters. Accurate CPU-efficient numerical methods and semi-analytical solutions may have a clear advantage for the corresponding comparative study. Employing these solutions makes it possible to get fundamental information on the eigen (or characteristic forced) oscillations and, thereby, estimate applicability of the aforementioned physical models. Getting these accurate approximate solutions is also useful for *verification* of more universal numerical schemes, debugging and testing convergence of the codes based, for instance, on the Finite Element Method.

A typical composite mechanical system may consist of a central flexible object and one or two rigid bodies attached to the ends of this object. The central object should be considered as either beam or cylindrical shell, but the attached bodies can be associated with either point masses or rigid bodies. Idealizing to the point masses or the rigid bodies yields the simplest situation from physical (degrees of freedom, physical phenomena, etc.) and mathematical (governing equations, transmission and boundary conditions, etc.) points of view. There is the wide literature on this topic. One could refer to Forsberg (1966) who studied oscillations of two heavy rigid-ring bodies attached to a circular cylindrical weightless shell. Further, Bukharinov (1974) accounted for the shell weight, but suggested additionally that the rigid bodies have equal masses. A free shell having a single stiffening ring at its end was considered by Sharma and Johns (1966, 1968, 1970, 1971). They assumed that the ring is made from the same material as the shell. Longitudinal and torsional oscillations of a circular cylindrical shell with two point masses clamped to its ends were also investigated by Breslavsky (1973, 1981). Trotsenko and Kladinoga (1994) studied the coupled eigenoscillations of a prestressed hyperelastic shell of revolution and a rigid disk attached to one of the shell ends. The encyclopedia-book by Leissa (1993) refers also to (i) eigenoscillations of a rigid-ring body attached to the shell end, and (ii) vibrations of a shell with a rigid mass incorporated into the shell body as the most popular study cases related to the idealization. The current state-of-the-art on linear and nonlinear vibrations of a circular cylindrical shells with attached rigid

* Corresponding author. Tel.: +47 73 59 55 24.
E-mail address: alexander.timokha@ntnu.no (A. Timokha).

0020-7683/$ - see front matter © 2010 Elsevier Ltd. All rights reserved.
doi:10.1016/j.ijsolstr.2010.03.021

bodies can be found in the paper by Pellicano (2007) who proposed a solution method based on the Sanders–Koiter theory. Pellicano (2007) has also considered different boundary conditions as well as types of coupling with rigid bodies. His results were supported by model tests.

The present paper primary concentrates on the case, when the attached bodies are long and flexible, namely, they cannot generally be considered the rigid bodies, but rather beams. This is relevant to macroelements of multi-stage launch vehicles (Kiefling and Leadbetter, 1971), pipelines, constructive elements of bridges and offshore structures (Rotter, 1998, and references cited therein) as well as to embedding nanotubes (Legoas et al., 2004; Gibson et al., 2007). The coupled oscillations of these composite mechanical system can then be modeled by considering either the beam–shell–beam (BSB, or SB, shell–beam) or, under certain circumstances, the beam–beam–beam (BBB, or BB, beam–beam) mechanical system. An illustrative comparative study of these systems in terms of the eigenfrequencies and modes versus several nondimensional input parameters is a *particular goal* of the present paper. Forced oscillations can also be examined by using similar approximate methods, but, in the authors' opinion, those dedicated studies should be done within the framework of another presentation.

Accurate and CPU-efficient analytically oriented methods providing this study is *another important goal*. These methods can be considered an alternative to the Finite Element Method (FEM), e.g. packages ANSIS and NASTRAN. The accuracy is confirmed by numerous computational experiments; the corresponding fast convergence is exemplified in Section 3.

Historically, this double-goal problem was stated by engineers who deal with a certain class of composite constructions consisting of a large number of joint BBB/BSB-type components. Originally, using standard criteria, they have realised that the components can be modeled by the BBB-system. The corresponding software was developed, and it was showed that it is numerical efficient and, generally, applicable for computations of the whole composite construction. However, as it was told us, there were found situations for which the numerical results are not consistent with experimental data. Depending on the length, position of the central element, several components behaved like a BSB-system. The double task was stated. First, we had to give *a priori* estimate (by an exhaustive search through all the components) whether or not they can be described by the BBB-model. Second, after finding a component which requires the shell model for the central element, we had to advice the corrector factors in the input bending stiffness for the used software providing more adequate numerical output. Obviously, because thousands combinations should be tested, our method must be very CPU-efficient. In addition, it should be quite accurate to get not only qualitative conclusion on the used model, but also quantify the difference and compute the aforementioned corrector factors.

The literature survey showed us that Shveiko et al. (1968) is, most probably, the only paper which deals with the eigenproblem for the BSB-system providing, in fact, an analytical solution of this problem. Shveiko et al. (1968) approximated the eigensolution of the BSB-system by employing an exact solution of the Donnell–Mushtari–Vlasov equation. Discussing advantages and disadvantages of this analytical solution method, Trotsenko (2002) remarked that even though Shveiko et al. (1968) give an analytical, very accurate solution, its numerical realization is CPU-demanding, even if we compare it with the FEM. Thus, it cannot be used for solving the double task. Trotsenko (2002) assumed that an alternative could be a variational method with appropriate functional basis. The present paper constructs this functional basis, and employs it in a Ritz scheme. Some interesting properties of the BSB (compared with BBB) system (related to the case by Shveiko et al. (1968)) are emphasized. The focus is on dependencies of the eigenfrequencies and modes on the *nondimensional shell thickness, length and position* relative to the two attached beams. Remembering for the qualitative fact that the eigenfrequencies of the BSB-system are lower of those for the BBB-system, we focus on quantification of the eigenfrequencies versus as we mentioned, the shell thickness, length and its position between two, generally, non-equal beams. In addition, we show a sufficient difference between the eigenmodes. The difference may also matter for the cases when the eigenfrequencies of these two systems remain close to each other.

In Section 2, the governing equations and the boundary [transmission] conditions are formulated. These are taken from the paper by Shveiko et al. (1968) and, alternatively, they are derived by using the variational principle stating the equivalence of variations of the potential energy due to small deviations of the system to the corresponding virtual work done by the inertia forces. Details of this derivation are presented in Appendix A. Furthermore, we consider the problem on eigenoscillations of the BSB-system that appears as a spectral boundary problem. In Section 3, we construct a Ritz scheme for this spectral boundary problem utilizing variational statement from Appendix A. The method for the spectral problem on eigenoscillations of the BBB-system is also considered.

The comparative studies of BSB- and BBB-systems need to evaluate eigenfrequencies and eigenmodes versus numerous nondimensional input parameters. For brevity, the studies are related to the case by Shveiko et al. (1968) who considered a set of restrictions to the input nondimensional parameters; the relations are associated with a military spacecraft application. The three remaining independent input parameters can be related to the length of the central object, position of this object and the shell thickness. In Section 4, we analyze dependencies of eigenfrequencies and eigenmodes on these three parameters. In addition, the paper presents a comparative study of two-component systems consisting of shell–beam (SB) and shell–rigid body (SrB).

2. Statement

2.1. Introductory remarks and definitions

We consider small-amplitude oscillations of the mechanical system consisting of a circular cylindrical shell (in its unperturbed state of radius R, length l and thickness h) and two beams attached to the shell ends as shown in Fig. 1. This BSB-system is assumed to be symmetric relative to two mutually perpendicular planes,

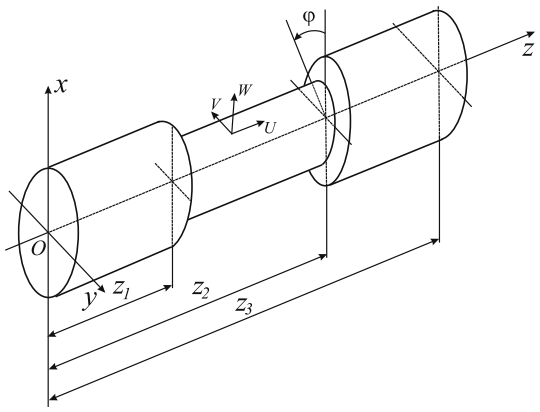

Fig. 1. Sketch of the BSB-system. Definition of the angle φ, as well as of the displacement V is in the negative direction, based on the choice of the orientation of the coordinate system $Oxyz$. This negative direction was used by Shveiko et al. (1968) who published the pioneering paper on the BSB-system.

whose intersection coincides with longitudinal axis of the circular cylindrical shell and the beams. We introduce the Cartesian coordinate system $Oxyz$ with the unit vectors $\mathbf{i}$, $\mathbf{j}$ and $\mathbf{k}$ so that the coordinate planes Oxz and Oyz are superposed with the perpendicular symmetry planes and the origin O lies on a beam end. Fig. 1 introduces z_1, z_2 and z_3, where z_3 is the total length of the BSB-system, z_1 is length of the first beam (touching the Oxy-plane), $z_2 = l + z_1$ and $z_3 - z_2 = z_3 - z_1 - l$ is length of the second beam.

The mean shell surface (mid-surface) deviates relative to its static cylindrical shape Σ. The mid-surface can be described in curvilinear (cylindrical) coordinate system $Ozr\varphi$, where the polar angle φ is positive in the counterclockwise direction when watching along the positive direction of the Oz-axis. In the $Ozr\varphi$-coordinate system, the small structural deviations are presented by the vector

$$\mathbf{U}(z,\varphi,t) = u(z,\varphi,t)\mathbf{e}_1 + v(z,\varphi,t)\mathbf{e}_2 + w(z,\varphi,t)\mathbf{e}_3, \quad z_1 < z < z_2, \quad 0 < \varphi \leqslant 2\pi. \tag{1}$$

Here, $\mathbf{e}_1$, $\mathbf{e}_2$ and $\mathbf{e}_3$ are the unit vectors of the $u - v - w$ natural coordinate system introduced on Σ as shown in Fig. 1. Vectors $\mathbf{e}_1$ and $\mathbf{e}_2$ are tangential to the coordinate curves of φ and z, respectively; $\mathbf{e}_3 = [\mathbf{e}_1 \times \mathbf{e}_2]$. Functions u, v and w are unknown and must be found from the linearized shell equations. The unknowns u, v and w depend on $z \in [z_1, z_2]$ and $\varphi \in [0, 2\pi]$. Obviously, u, v and w are 2π-periodic of the angular coordinate φ.

The small-amplitude beam vibrations are associated with instant deformations of its longitudinal axis which coincides with the Oz-axis in the unperturbed state. Without loss of generality, we consider only deformations in the Oxz-plane. The instant deformations of the two beams can then be modeled by functions $\xi_1(z,t)$ and $\xi_2(z,t)$ defined on intervals $[0, z_1]$ and $[z_2, z_3]$, respectively. These functions determine two planar curves in the Oxz-plane; these imply deviations of their longitudinal axes.

In summary, the small-amplitude coupled vibrations of the BSB-system occurring in the Oxz-plane are governed by the five unknowns

$$\begin{cases} \xi_1(z,t), & 0 < z < z_1, \\ u(z,\varphi,t), v(z,\varphi,t), w(z,\varphi,t), & z_1 < z < z_2, \quad 0 < \varphi \leqslant 2\pi, \\ \xi_2(z,t), & z_2 < z < z_3. \end{cases}$$

2.2. Boundary value problem

2.2.1. Geometric boundary- and transmission-conditions

At $z = z_1$ and $z = z_2$, the shell is rigidly fixed with the beam ends. Because these ends are flat and perpendicular to the Oz-axis, the contact points constitute two circles of radius R in the static state. The contact circles should deviate together with the beams and the shell. These deviations have to satisfy the relation

$$\mathbf{U}(z,\varphi) = \mathbf{U}_0 + [\theta_0 \times \mathbf{r}_0] \quad \text{at } z = z_1, z_2, \tag{2}$$

where $\mathbf{U}_0$ and θ_0 are vectors of small translatory and angular displacements of the beam ends at $z = z_1$ and $z = z_2$, respectively, and $\mathbf{r}_0$ is the corresponding radius-vectors of the shell ends with respect to the points $(0,0,z_k)$, $k = 1,2$. In the Cartesian coordinate system, the vectors $\mathbf{U}_0$, θ_0 and $\mathbf{r}_0$ are as follows:

$$\mathbf{U}_0 = \{\xi_k(z_k,t), 0, 0\}; \quad \theta_0 = \left\{0, \frac{d\xi_k(z_k,t)}{dz}, 0\right\};$$
$$\mathbf{r}_0 = \{R\cos\varphi, -R\sin\varphi, 0\}. \tag{3}$$

This implies that the right-hand side of (2) is a function of Dirichlet's and Neumann's traces of ξ_1 and ξ_2 on $z = z_1$ and $z = z_2$, respectively.

In turn, the left-hand side of Eq. (2) is expressed in terms of functions u, v and w. To find these expressions, we can use the following dependencies between the local basis $\mathbf{e}_1$, $\mathbf{e}_2$ and $\mathbf{e}_3$ (at the shell ends) and the Cartesian unit vectors $\mathbf{i}$, $\mathbf{j}$ and $\mathbf{k}$

$$\mathbf{i} = -\sin\varphi\mathbf{e}_2 + \cos\varphi\mathbf{e}_3; \quad \mathbf{j} = -\cos\varphi\mathbf{e}_2 - \sin\varphi\mathbf{e}_3; \quad \mathbf{k} = \mathbf{e}_1. \tag{4}$$

Substituting Eq. (4) into Eq. (1) and using the obtained result (together with (3)) in Eq. (2) yields the three geometric transmission conditions between u, v, w and ξ_k

$$u(z_k,\varphi,t) = -\frac{\partial\xi_k(z_k,t)}{\partial z}R\cos\varphi; \quad v(z_k,\varphi,t) = -\xi_k(z_k,t)\sin\varphi,$$
$$w(z_k,\varphi,t) = \xi_k(z_k,t)\cos\varphi \quad \text{at } z = z_k, \ k = 1,2. \tag{5}$$

Furthermore, local deformations at the shell ends have to keep invariant the right contact angle between the shell and the beams flat ends. Earlier, we assumed (for brevity) that the beams [their longitudinal axes] oscillate in the Oxz-plane. Under this assumption, the mentioned invariance means that the beam ends perform angular motions around the unit vector $\mathbf{e}_2$. As a result, the additional geometrical transmission condition are

$$\frac{\partial w(z_k,\varphi,t)}{\partial z} = \frac{\partial\xi_k(z_k,t)}{\partial z}\cos\varphi, \quad k = 1,2. \tag{6}$$

There are also the geometric boundary conditions that are formulated at the beam ends $z = 0$ and $z = z_3$. Usually, these are either the clamped-end condition

$$\xi_j = \frac{\partial\xi_j}{\partial z} = 0 \quad \text{at } z = 0 \quad \text{or} \quad z = z_3; \quad j = 1,2, \tag{7}$$

or the free-end condition

$$\frac{\partial^2\xi_j}{\partial z^2} = \frac{\partial^3\xi_j}{\partial z^3} = 0 \quad \text{at } z = 0 \quad \text{or} \quad z = z_3; \quad j = 1,2. \tag{8}$$

2.2.2. Governing equations and dynamic transmission conditions

Let us denote the beam mass per its length (linear mass) and the flexural rigidities of the beams as $m_k(z)$ and $E_kI_k(z)$, respectively, so that $k = 1$ corresponds to the first beam with $z \in [0, z_1]$ and $k = 2$ implies the second beam with $z \in [z_2, z_3]$. The governing equations for shell and two beams as well as the corresponding dynamic transmission conditions at $z = z_k$, $k = 1,2$, which reflect balance of forces and moments, can be taken from the paper by Shveiko et al. (1968), or, alternatively, derived by using a variational principle (see, Appendix A). The governing equations are as follows:

$$\begin{aligned} &L_{11}(u) + L_{12}(v) + L_{13}(w) = \frac{\rho(1-\nu^2)}{E}\frac{\partial^2 u}{\partial t^2}, \\ &L_{21}(u) + L_{22}(v) + L_{23}(w) = \frac{\rho(1-\nu^2)}{E}\frac{\partial^2 v}{\partial t^2}, \\ &L_{31}(u) + L_{32}(v) + L_{33}(w) = -\frac{\rho(1-\nu^2)}{E}\frac{\partial^2 w}{\partial t^2}, \\ &\frac{\partial^2}{\partial z^2}\left(E_kI_k\frac{\partial^2\xi_k}{\partial z^2}\right) + m_k\frac{\partial^2\xi_k}{\partial t^2} = 0, \quad k = 1,2, \end{aligned} \tag{9}$$

where

$$\begin{aligned} &L_{11} = \frac{\partial^2}{\partial z^2} + \frac{v_1}{R^2}\frac{\partial^2}{\partial\varphi^2}; \quad L_{12} = L_{21} = \frac{v_2}{R}\frac{\partial^2}{\partial z\partial\varphi}; \\ &L_{13} = L_{31} = \frac{v}{R}\frac{\partial}{\partial z}, \\ &L_{22} = \frac{1}{R^2}\frac{\partial^2}{\partial\varphi^2} + v_1\frac{\partial^2}{\partial z^2}; \quad L_{23} = L_{32} = \frac{1}{R^2}\frac{\partial}{\partial\varphi}; \\ &L_{33} = \frac{1}{R^2}(c^2\Delta\Delta + 1), \\ &\Delta = R^2\frac{\partial^2}{\partial z^2} + \frac{\partial^2}{\partial\varphi^2}; \quad v_1 = \frac{1-\nu}{2}; \quad v_2 = \frac{1+\nu}{2}; \quad c^2 = \frac{h^2}{12R^2} \end{aligned} \tag{10}$$

and E_k is Young's modulus.

According to Shveiko et al. (1968), the dynamic transmission and shell-ends boundary conditions take the form

$$\int_\Gamma (S\sin\varphi - Q_1^*\cos\varphi)\big|_{z=z_k}\,ds - Q^{(k)}\Big|_{z=z_k} = 0, \tag{11a}$$

$$\int_\Gamma (T_1 R\cos\varphi + M_1\cos\varphi)\big|_{z=z_k}\,ds + M^{(k)}\Big|_{z=z_k} = 0, \quad k=1,2, \tag{11b}$$

where T_1 and S are the stretch (along the meridians) and the shear force (referred to the unit length of the cross-section of the mean shell surface Σ), respectively; Q_1^* is the generalized cross-force applied to the shell contour, M_1 is the linear bending moment in the shell meridional plane, $M^{(k)}$ and $Q^{(k)}$ are the bending moment and the shear force for the two beams. The latter values are represented by the formulas

$$\begin{aligned}
&S = \frac{Eh}{2(1+\nu)}\left(\frac{\partial v}{\partial z} + \frac{1}{R}\frac{\partial u}{\partial\varphi}\right); \quad T_1 = \frac{Eh}{1-\nu^2}\left[\frac{\partial u}{\partial z} + \frac{v}{R}\left(\frac{\partial v}{\partial\varphi} + w\right)\right],\\
&M_1 = -D\left(\frac{\partial^2 w}{\partial z^2} + \frac{\nu}{R^2}\frac{\partial^2 w}{\partial\varphi^2}\right),\\
&Q_1^\star = -c^2\frac{Eh}{1-\nu^2}\left[R^2\frac{\partial^3 w}{\partial z^3} + (2-\nu)\frac{\partial^3 w}{\partial z\partial\varphi^2}\right],\\
&M^{(k)} = E_k I_k\frac{\partial^2\xi_k}{\partial z^2}; \qquad Q^{(k)} = \frac{\partial}{\partial z}\left(E_k I_k\frac{\partial^2\xi_k}{\partial z^2}\right), \quad k=1,2.
\end{aligned} \tag{12}$$

Eqs. (11) imply the fact that the resulting force (projection on the Ox-axis) and the moment (relative to the Oy-axis) are zero at the contact contours.

In summary, motions of the BSB-system are described by the governing equations (9) with geometric (5) and (6) and dynamic (11) transmission conditions and the clamped-end (7) or the free-end (8) condition.

2.3. Eigenfrequencies and eigenmodes

Henceforth, linear problem (9), (5), (6), (11) and ((7) or (8)) is nondimensionalized and considered in the cylindrical coordinate system. The main focus is the eigenoscillations, i.e. we consider the $\exp(i\omega t)$-proportional solution

$$\begin{aligned}
&u = e^{i\omega t}u_n(z)\cos n\varphi; \quad v = e^{i\omega t}v_n(z)\sin n\varphi; \quad w = e^{i\omega t}w_n(z)\cos n\varphi,\\
&\xi_k = e^{i\omega t}\eta_k(z), \quad n=1,2,\ldots; \quad k=1,2,\ i^2=-1;
\end{aligned} \tag{13}$$

forces and moments associated with shell deformations are defined by

$$\begin{aligned}
&T_1 = e^{i\omega t}T_{1(n)}\cos n\varphi; \quad T_2 = e^{i\omega t}T_{2(n)}\cos n\varphi; \quad S = e^{i\omega t}S_{(n)}\sin n\varphi,\\
&Q_1^\star = e^{i\omega t}Q_{1(n)}^\star\cos n\varphi; \quad M_1 = e^{i\omega t}M_{1(n)}\cos n\varphi.
\end{aligned} \tag{14}$$

The normalization adopts the characteristic dimension R and time $\sqrt{E/((1-\nu^2)\rho R^2)}$ which lead to the following nondimensional parameters:

$$\gamma_1 = \frac{z_1}{R}; \quad \gamma_2 = \frac{z_3 - z_2}{R}; \quad \gamma = \frac{l}{R}, \tag{15a}$$

$$\alpha_1 = \frac{z}{R}; \quad \alpha_2 = \frac{z_3 - z}{R}; \quad \alpha = \frac{z - z_1}{R}, \tag{15b}$$

$$\{\bar u_n, \bar v_n, \bar w_n\} = R^{-1}\{u_n, v_n, w_n\}, \tag{15c}$$

$$\left\{\overline{T}_{1(n)}, \overline{Q}^\star_{1(n)}, \overline{S}_{(n)}\right\} = \frac{(1-\nu^2)}{Eh}\left\{T_{1(n)}, Q^\star_{1(n)}, S_{(n)}\right\}, \tag{15d}$$

$$\overline{M}_{1(n)} = \frac{(1-\nu^2)}{EhR}M_{1(n)}; \quad \overline{Q}^{(k)} = \frac{1}{\pi EhR}Q^{(k)}; \quad \overline{M}^{(k)} = \frac{1}{\pi EhR^2}M^{(k)}, \tag{15e}$$

$$\bar\omega^2 = \frac{(1-\nu^2)\rho R^2}{E}\omega^2; \quad \zeta_k = \frac{E_k I_k}{\pi EhR^3}; \quad \bar m_k = \frac{m_k}{(1-\nu^2)\pi\rho Rh}. \tag{15f}$$

Here, Eq. (15a) defines the nondimensional lengths of the beams and the shell, Eq. (15b) introduces the local 'nondimensional' longitudinal axes for the beams and the shell, Eq. (15c) presents nondimensional deviations of the shell associated with nth eigenmode, $\left\{\overline{T}_{1(n)}, \overline{S}_{(n)}, \overline{Q}^\star_{1(n)}, \overline{M}_{1(n)}\right\}$ are nondimensional stretch and shear forces, nondimensional generalized cross-force and linear bending moment for the shell (associated with nth eigenmode), respectively, and $\overline{Q}^{(k)}$ and $\overline{M}^{(k)}$ are the nondimensional bending moment and shear force for kth beam, respectively. Eq. (15f) introduces the nondimensional eigenfrequency $\bar\omega$, the nondimensional bending stiffness for kth beam, ζ_k, and the nondimensional structural mass, $\bar m_k$ for the two beams $k=1,2$. Whereas the normalization of the shell-related parameters is associated with a standard procedure, we should emphasis the nondimensional parameters of the beams, $\overline{Q}^{(k)}$, $\overline{M}^{(k)}$, ζ_k and $\bar m_k$, $k=1,2$ whose normalization is obtained by scaling them by those for the shell.

Omitting overbars in the nondimensional parameters, we get the n-parametric family of the ODE coupling $u_n(\alpha)$, $v_n(\alpha)$, $w_n(\alpha)$ and $\eta_k(\alpha_k)$ (eigenmodes) and eigenfrequency ω

$$\frac{d^2}{d\alpha_k}\left(\zeta_k\frac{d^2\eta_k}{d\alpha_k^2}\right) - \omega^2 m_k\eta_k = 0, \tag{16}$$

$$\begin{aligned}
&L_{11}^{(n)}(u_n) + L_{12}^{(n)}(v_n) + L_{13}^{(n)}(w_n) + \omega^2 u_n = 0,\\
&L_{21}^{(n)}(u_n) + L_{22}^{(n)}(v_n) + L_{23}^{(n)}(w_n) + \omega^2 v_n = 0,\\
&L_{31}^{(n)}(u_n) + L_{32}^{(n)}(v_n) + L_{33}^{(n)}(w_n) - \omega^2 w_n = 0, \quad n=1,2,\ldots; \quad k=1,2.
\end{aligned} \tag{17}$$

Here, $L_{ij}^{(n)}$, $i,j=1,\ldots,3$ are differential operators obtained from operators L_{ij} by separating the angular variable φ. The boundary conditions for the free- or clamped beam ends (in nondimensional formulation, at $\alpha_1=0$ and $\alpha_2=0$) should also be added.

Substituting (13) into transmission conditions (11) gives different results for $n=1$ and $n\neq 1$. When $n=1$, the transmission conditions take the form

$$\begin{aligned}
&u_1(\chi_k) = (-1)^k\frac{d\eta_k(\gamma_k)}{d\alpha_k}; \quad \frac{dw_1(\chi_k)}{d\alpha} = (-1)^{k+1}\frac{d\eta_k(\gamma_k)}{d\alpha_k},\\
&v_1(\chi_k) = -\eta_k(\gamma_k); \quad w_1(\chi_k) = \eta_k(\gamma_k),
\end{aligned} \tag{18}$$

$$\begin{aligned}
&\left\{c^2\left[\frac{d^3 w_1}{d\alpha^3} - (2-\nu)\frac{dw_1}{d\alpha}\right] + v_1\left(\frac{dv_1}{d\alpha} - u_1\right)\right\}_{\alpha=\chi_k}\\
&\quad + (-1)^k(1-\nu^2)\frac{d}{d\alpha_k}\left(\zeta_k\frac{d^2\eta_k}{d\alpha_k^2}\right)_{\alpha_k=\gamma_k} = 0,
\end{aligned} \tag{19a}$$

$$\begin{aligned}
&\left[c^2\left(\nu w_1 - \frac{d^2 w_1}{d\alpha^2}\right) + \frac{du_1}{d\alpha} + \nu(v_1 + w_1)\right]_{\alpha=\chi_k}\\
&\quad + (1-\nu^2)\left(\zeta_k\frac{d^2\eta_k}{d\alpha_k^2}\right)_{\alpha_k=\gamma_k} = 0, \quad k=1,2,
\end{aligned} \tag{19b}$$

where $\chi_1=0$ and $\chi_2=\gamma$. In contrast, when $n>1$, the transmission conditions transform to the form

$$u_n(\chi_k) = v_n(\chi_k) = w_n(\chi_k) = \frac{dw_n(\chi_k)}{d\alpha} = 0, \quad k=1,2. \tag{20}$$

The difference between conditions (19) and (20) means that the eigenmodes of the BSB-system fall into two types. The first type

(*beam-type motions*, $n = 1$ Forsberg, 1966) is associated with a non-trivial solution of Eqs. (16)–(19) and ((7) or (8)). The first-type eigenmodes represent the coupled shell–beams oscillations imposing that all the functions u_1, v_1, w_1 and η_1, η_2 are not zero. However, in view of representation (14), projections of the resulting force on axes Oy and Oz, the bending moment around the Ox-axis and the torsion moment, which are transferred from shell to beams, are then equal to zero. This means that these eigenmodes imply transverse motions of the beams in the Oxz-plane. In contrast, the second-type solution ($n \neq 1$) means the uncoupling between u_n, v_n, w_n and η_k so that the shell performs oscillations in the Oxz-plane, but the two beams remain motionless.

3. Approximate eigenfrequencies and eigenmodes

3.1. The Ritz scheme for the BSB-system

When the shell thickness and other characteristics are constant values, Shveiko et al. (1968) found an analytical solution of Eq. (17) within a fixed value of ω. Employing this solution as well as the solution of the beam equation (16) (with the same fixed frequency ω), they used conditions (18) and (19) (together with the clamped-end condition (7)) to derive a linear homogeneous algebraic system of the twelfth order with respect to a full set of the unknown integration variables. The eigenmode corresponds to a non-trivial solution of the linear algebraic system. Coefficients of the corresponding matrix are a function of ω. To find the eigenfrequencies, Shveiko et al. (1968) used the zero-determinant condition considered with respect to ω. The roots may be computed by diverse iterative methods. Trotsenko (2002) reexamined the method by Shveiko et al. (1968). He reported a series of misprints and showed that the analytical solution of (17) by Shveiko et al. (1968) can reasonably change its properties with varying ω and geometric and physic parameters. As a consequence, numerical realization of the method may become difficult and in many cases unstable. The variational scheme from this section can be considered an alternative.

Our analysis uses expressions from Appendices A and B. After separation of t and φ (due to (13)), the original spectral problem can be considered the necessary extrema condition of the functional

$$\begin{aligned} I = \frac{1}{2}\int_0^{\gamma}\Bigg[&\left(\frac{du_n}{d\alpha}\right)^2 + (w_n + n v_n)^2 + 2\nu\frac{du_n}{d\alpha}(w_n + n v_n) \\ &+ \nu_1\left(\frac{dv_n}{d\alpha} - n u_n\right)^2\Bigg]d\alpha + \frac{c^2}{2}\int_0^{\gamma}\Bigg[\left(\frac{d^2 w_n}{d\alpha}\right) + n^4 w_n^2 \\ &- 2\nu n^2\frac{d^2 w_n}{d\alpha^2}w_n + 2(1-\nu)n^2\left(\frac{dw_n}{d\alpha}\right)^2\Bigg]d\alpha \\ &+ \frac{(1-\nu^2)}{2}\sum_{k=1}^{2}\int_0^{\gamma_k}\zeta_k\left(\frac{d^2\eta_k}{d\alpha_k}\right)^2 d\alpha_k \\ &- \frac{\omega^2}{2}\left[\int_0^{\gamma}(u_n^2 + v_n^2 + w_n^2)d\alpha + (1-\nu^2)\sum_{k=1}^{2}\int_0^{\gamma_k} m_k\eta_k^2\, d\alpha_k\right]. \end{aligned} \tag{21}$$

When $n = 1$, this functional should be minimized with respect to functions which satisfy equations and boundary conditions (18) and the clamped- or free-end boundary conditions, namely, (7) or (8). The dynamic transmission condition (19) naturally follows from the minimization. For the case $n > 1$, the geometric transmission condition restricts functional (21) to relations $\eta_k \equiv 0$, $k = 1,2$. The statement needs also conditions (20).

For brevity of description, we assume that the two beams are rigidly fixed (clamped) at the ends, i.e. $\eta_j = 0$ at $\alpha_1 = \alpha_2 = 0$. Because

$$\frac{d^4\eta_k}{d\alpha_k^4} - \beta_k^4\eta_k = 0; \qquad \beta_k^4 = \frac{m_k\omega^2}{\zeta_k}, \quad k = 1,2, \tag{22}$$

the clamped-end conditions deduce the following analytical solution:

$$\begin{aligned} &\eta_1(\alpha_1) = C_1 U(\beta_1\alpha_1) + C_2 V(\beta_1\alpha_1); \\ &\eta_2(\alpha_2) = D_1 U(\beta_2\alpha_2) + D_2 V(\beta_2\alpha_2). \end{aligned} \tag{23}$$

Here, C_i and D_i, $i = 1,2$ are real numbers, and $U(\beta_i z)$ and $V(\beta_i z)$ are the so-called Krylov functions (Krylov, 1936)

$$U(\beta z) = \frac{1}{2}(\cosh\beta z - \cos\beta z), \quad V(\beta z) = \frac{1}{2}(\sinh\beta z - \sin\beta z).$$

The unknowns $u_n(\alpha)$, $v_n(\alpha)$ and $w_n(\alpha)$ are imposed to satisfy the transmission conditions. This can be done by assuming that

$$\begin{aligned} u_n(\alpha) &= \sum_{j=1}^{N} a_j U_j(\alpha) + \delta_{1n}\left(\frac{d\eta_2(\gamma_2)}{d\alpha_2}f_2(\alpha) - \frac{d\eta_1(\gamma_1)}{d\alpha_1}f_1(\alpha)\right), \\ v_n(\alpha) &= \sum_{j=1}^{N} b_j V_j(\alpha) - \delta_{1n}(\eta_1(\gamma_1)f_1(\alpha) + \eta_2(\gamma_2)f_2(\alpha)), \\ w_n(\alpha) &= \sum_{j=1}^{N} c_j W_j(\alpha) + \delta_{1n}\Bigg(\eta_1(\gamma_1)g_1(\alpha) + \eta_2(\gamma_2)g_2(\alpha). \\ &\quad + \frac{d\eta_1(\gamma_1)}{d\alpha_1}h_1(\alpha) - \frac{d\eta_2(\gamma_2)}{d\alpha_2}h_2(\alpha)\Bigg), \\ \delta_{1n} &= \begin{cases} 1, & \text{for } n = 1, \\ 0, & \text{for } n > 1, \end{cases} \end{aligned} \tag{24}$$

where a_j, b_j, c_j are arbitrary real numbers,

$$\begin{aligned} &f_1(\alpha) = 1 - \frac{\alpha}{\gamma}; \quad f_2(\alpha) = \frac{\alpha}{\gamma}; \quad g_1(\alpha) = 1 - \frac{3}{\gamma^2}\alpha^2 + \frac{2}{\gamma^3}\alpha^3, \\ &g_2(\alpha) = 1 - g_1(\alpha); \quad h_1(\alpha) = \alpha - \frac{2}{\gamma}\alpha^2 + \frac{1}{\gamma^2}\alpha^3; \quad h_2(\alpha) = -\frac{\alpha^2}{\gamma} + \frac{\alpha^3}{\gamma^2}, \end{aligned}$$

and the coordinate functions $U_j(\alpha)$, $V_j(\alpha)$ and $W_j(\alpha)$ have to satisfy condition (20). When $n = 1$, the terms in the front of the Kronecker delta provides the fulfillment of the transmission conditions (19) for the beam-type eigenoscillations.

Representations (23) and (24) yield the following vector formed by the unknown constants:

$$\mathbf{X} = \{a_1, a_2, \ldots, a_N, b_1, b_2, \ldots, b_N, c_1, c_2, \ldots, c_N, C_1, C_2, D_1, D_2\}.$$

One should note that representation (24) includes itself the eigenmodes which correspond to the eigenfrequencies ω_{1i}^* for which $\eta_1(\gamma_1) = d\eta_1(\gamma_1)/d\alpha_1 = 0$, and the eigenfrequencies $\omega_{2i}^\star$ providing $\eta_2(\gamma_2) = d\eta_2(\gamma_2)/d\alpha_2 = 0$. As long as a frequency ω coincides with ω_{1i}^*, the first beam satisfies the clamped-end condition at $\alpha_1 = 0$. The shell and the second beam remain motionless. Analogous situation occurs for $\omega_{2i}^\star$, i.e. the first beam and the shell are unmovable, but the second beam performs eigenoscillations. Furthermore, we exclude these cases from consideration and focus exclusively on the coupled eigenoscillations of the BSB-system. A way to do this consists of dividing the expressions for $\eta_1(\gamma_1)$, $d\eta_1\ (\gamma_1)/d\alpha_1$ and $\eta_2(\gamma_2)$, $d\eta_2(\gamma_2)/d\alpha_2$ by the coefficients

$$K_1 = \sum_{i=1}^{p}(\omega - \omega_{1i}^*); \quad K_2 = \sum_{i=1}^{p}(\omega - \omega_{2i}^*),$$

where ω_{1i}^* and ω_{2i}^* are found from the corresponding problems on the beam vibrations and integer p is chosen to overlap the tested range of ω.

Our choice of a set of linearly independent and complete functions on interval $[0,\gamma]$ is Legendre's polynomials. This means that

$$U_j(\alpha) = V_j(\alpha) = \alpha(\alpha-\gamma)P_j\left(\frac{2}{\gamma}\alpha - 1\right),$$
$$W_j(\alpha) = \alpha^2(\alpha-\gamma)^2 P_j\left(\frac{2}{\gamma}\alpha - 1\right), \quad j = 1,\dots,N, \tag{25}$$

where $P_j(z)$ are the Legendre polynomials, whose first two derivatives can be found by using the recurrent formulas

$$P_{j+2}(z) = \frac{1}{j+1}[(2j+1)zP_{j+1}(z) - jP_j(z)],$$
$$P'_{j+2}(z) = zP'_{j+1}(z) + (j+1)P_{j+1}(z),$$
$$P''_{j+2}(z) = zP''_{j+1}(z) + (j+2)P'_{j+1}(z),$$
$$P_1(z) = 1; \quad P_2(z) = z; \quad P_3(z) = \frac{1}{2}(3z^2-1).$$

In contrast to standard Ritz's scheme, representation (24) of $u_1(\alpha)$, $v_1(\alpha)$ and $w_1(\alpha)$ is nonlinearly dependent on the unknown parameters C_1, C_2 and D_1, D_2. This means that the homogeneous system with respect to $\mathbf{X}$ is generally speaking nonlinear. A simplification is possible based on a preliminary calculus of variations in functional (21) with accounting for transformations and special features of $\eta_1(\alpha_1)$ and $\eta_2(\alpha_2)$ that consist of particular solutions of the beam equation.

Let us introduce the following differential operators:

$$\Psi_{11}(p,q) = \frac{dp}{d\alpha}\frac{dq}{d\alpha} + \nu_1 n^2 pq; \quad \Psi_{12}(p,q) = \nu np\frac{dq}{d\alpha} - \nu_1 n\frac{dp}{d\alpha}q,$$
$$\Psi_{13}(p,q) = \nu p\frac{dq}{d\alpha}; \quad \Psi_{23}(p,q) = npq; \quad \Psi_{22}(p,q) = n^2pq + \nu_1\frac{dp}{d\alpha}\frac{dq}{d\alpha},$$
$$\Psi_{33}(p,q) = pq + c^2\left[\left(\frac{d^2p}{d\alpha^2} - \nu n^2 p\right)\frac{d^2q}{d\alpha^2} + \left(n^4 p - \nu n^2\frac{d^2p}{d\alpha^2}\right)q + 2(1-\nu)n^2\frac{dp}{d\alpha}\frac{dq}{d\alpha}\right], \tag{26}$$

where $p(\alpha)$ and $q(\alpha)$ are arbitrary functions. This presents variations of functional (21) as

$$\delta I = \int_0^\gamma [\Psi_{11}(u_n,\delta u_n) + \Psi_{12}(v_n,\delta u_n) + \Psi_{13}(w_n,\delta u_n) + \Psi_{12}(\delta v_n,u_n) + \Psi_{22}(v_n,\delta v_n) + \Psi_{23}(w_n,\delta v_n) + \Psi_{13}(\delta w_n,u_n) + \Psi_{23}(\delta w_n,v_n) + \Psi_{33}(w_n,\delta w_n)]d\alpha - \omega^2\int_0^\gamma (u_n\delta u_n + v_n\delta v_n + w_n\delta w_n)d\alpha + (1-\nu^2)\sum_{k=1}^{2}\left[\zeta_k\frac{d^2\eta_k}{d\alpha_k^2}\frac{d\delta\eta_k}{d\alpha_k} - \frac{d}{d\alpha_k}\left(\zeta_k\frac{d^2\eta_k}{d\alpha_k^2}\right)\delta\eta_k\right]_{\alpha_k=\gamma_k}. \tag{27}$$

The components of $\mathbf{X}$ are determined from the necessary extrema condition of the functional. This transforms the original problem to the generalized eigenvalue problem

$$(A - \omega^2 B)\mathbf{X}^T = 0, \tag{28}$$

where A and B are symmetric matrices of the order $3N+4$ for $n=1$ and $3N$ for $n>1$. Some elements of A and B depend on the frequency ω because it is presented in terms of Krylov's functions. Expressions for elements of matrices A and B are presented in Appendix B.

When $n>1$, the matrices A and B can be constructed by involving elements of the matrices of the case $n=1$ by crossing out the last four rows and columns. Hence, approximate solutions on the eigenoscillations of the BSB-system reduce to calculation of a series of integrals and identification of the eigenvalues from the matrix spectral problem (28).

Trotsenko (2006) considered the coupled free oscillations of a cylindrical shell with an attached rigid body at its end. Another end of the shell was rigidly clamped. Employing the methods above, one can compare these results with those when the attached body is a beam. For the clamped end of the shell, the following boundary conditions should be fulfilled:

$$u_1(\chi_1) = v_1(\chi_1) = w_1(\chi_1) = \left.\frac{dw_1(\alpha)}{d\alpha}\right|_{\alpha=\chi_1} = 0. \tag{29}$$

The transmission condition at $\alpha_2 = 0$ is

$$\frac{d^2\eta_2(\alpha_2)}{d\alpha_2^2} = \left.\frac{d^3\eta_2(\alpha_2)}{d\alpha_2^3}\right|_{\alpha_2=0} = 0. \tag{30}$$

In summary, we have

$$\eta_2(\alpha_2) = D_1 S(\beta_2\alpha_2) + D_2 T(\beta_2\alpha_2).$$

One can see that to get the final computational formulas, it is enough to exclude the rows and columns $3N+1$, $3N+2$ in matrices A, B in Eq. (28). The formulas for coefficients $C^2_{i,j}$, $(i,j=1,2)$ need the following formal substitution $\{S,T,U,V\} \to \{U,V,S,T\}$.

The modified method was tested to approximate the eigenfrequencies and the eigenmodes for the case of the clamped beam ends. The nondimensional parameters (45) are adopted. Length and thickness of the cylindrical shell varied. Elements of matrices A and B are computed by using the Gauss quadratures.

Tables 1 and 2 illustrate typical convergence to the five lower eigenfrequencies versus N in representation (24) with $\gamma=2$, $\gamma_1=8$, $\zeta=2$ and $\gamma=6$, $\gamma_1=4$, $\zeta=2$. The results show a fast convergence and good accuracy (five significant figures are stabilized) for an intermediate shell length. Longer shells need larger N in representation (24) to get the same accuracy. All the stabilized significant figures were controlled by comparing with the benchmark analytical solution by Shveiko et al. (1968). The comparison established that these stabilized significant figures coincide with those by Shveiko et al. (1968) and, thereby, we confirmed quite good accuracy of the method. The eigenfunctions by the method are also very close to the analytical solution by Shveiko et al. (1968) providing 3–5 significant figures in the uniform metrics in the case when 5–6 significant figures of the eigenvalues are stabilized.

Computations remain robust and can provide larger number of significant figures with larger N that does not exceed the polynomial degree $N=40$. For $N \geqslant 50$, the matrices may, however, become ill-conditioned and special modifications of the method, e.g. Gramm–Schmidt orthogonalization, is needed to get it stable.

3.2. The BBB-system

We assume that cross-sections of the shell remain flat and perpendicular to its neutral axis and the normal stresses (parallel of this axis) are negligible. In this case, the shell can theoretically be replaced by an equivalent beam, whose linear mass $m = 2\pi Rh\rho$ and the bending rigidity $EI = E\pi R^3 h$ are constant values. As a result, the problem reduces to identifying the eigenoscillations of a heterogeneous elastic beam with the piecewise bending rigidity $E_i I_i$ and linear mass m_i. A solution method for this problem may consist of shooting numerical procedure with the initial Cauchy conditions (see Krylov, 1936). This procedure makes it possible to determine

Table 1
Numerical values of the five lowest eigenfrequencies versus the number N of coordinate functions for $\gamma=2$, $\gamma_1=8$ and $\zeta=2$.

N	ω_1	ω_2	ω_3	ω_4	ω_5
2	0.03813	0.09778	0.19468	0.29943	0.44334
4	0.03810	0.09772	0.19462	0.29933	0.44279
6	0.03809	0.09770	0.19460	0.29931	0.44275
8	0.03808	0.09770	0.19460	0.29931	0.44274
10	0.03808	0.09770	0.19459	0.29931	0.44274

Table 2
Numerical values of the five eigenfrequencies versus the number N of coordinate functions for $\gamma = 6$, $\gamma_1 = 4$ and $\zeta = 2$.

N	ω_1	ω_2	ω_3	ω_4	ω_5
2	0.03885	0.10514	0.18342	0.29362	0.38854
4	0.03873	0.10353	0.18275	0.26800	0.38800
6	0.03870	0.10343	0.18271	0.26745	0.38704
8	0.03868	0.10341	0.18269	0.26727	0.38690
10	0.03867	0.10340	0.18268	0.26720	0.38686
12	0.03866	0.10339	0.18267	0.26716	0.38684
14	0.03866	0.10339	0.18267	0.26716	0.38684

eigenfrequencies and eigenmodes by using the so-called frequency determinant, whose order is independent of the mode number. The method is CPU-efficient, because it reduces to multiplying matrices of the fourth order and computations of the roots of a transcendental equation.

Let us divide a beam into k subsections with the lengths l_i, $i = 1,\ldots,k$. The bending rigidity and linear mass are constant values on each of these subsections. We introduce the corresponding coordinate systems for these subsections. This gives the following differential equations with constant coefficients:

$$\frac{d^4\eta_i(z_i)}{dz_i^4} - \beta_i^4\eta_i(z_i) = 0; \quad \beta_i^4 = \frac{m_i}{D_i}\omega^2; \quad D_i = E_iI_i, \quad 0 \leqslant z_i \leqslant l_i, \quad i = 1,\ldots,k, \tag{31}$$

where ω is eigenfrequency, $\eta_i(z_i)$ is eigenmode for ith subsection.

Eq. (31) needs both transmission and boundary conditions. The transmission conditions between each of ith and $i+1$th subsections are

$$\eta_i(l_i) = \eta_{i+1}(0); \quad \eta_i'(l_i) = \eta_{i+1}'(0); \quad D_i\eta_i''(l_i) = D_{i+1}\eta_{i+1}''(0), \quad D_i\eta_i'''(l_i) = D_{i+1}\eta_{i+1}'''(0). \tag{32}$$

These reflect the continuity of the flexure, the angular displacement, the bending moments and the cross-cutting forces. The general solution for each subsection can be presented as

$$\eta_i(z_i) = \eta_i(0)S(\beta_iz_i) + \frac{1}{\beta_i}\eta_i'(0)T(\beta_iz_i) + \frac{1}{\beta_i^2}\eta_i''(0)U(\beta_iz_i) + \frac{1}{\beta_i^3}\eta_i'''(0)V(\beta_iz_i). \tag{33}$$

Let us introduce the four-dimensional vector

$$\mathbf{u}_i(z_i) = \{u_{1i}, u_{2i}, u_{3i}, u_{4i}\}^T,$$

whose components are related to functions $\eta_i(z_i)$ and their derivative by

$$u_{1i} = \eta_i(z_i); \quad u_{2i} = \eta_i'(z_i); \quad u_{3i} = D_i\eta_i''(z_i); \quad u_{4i} = D_i\eta_i'''(z_i). \tag{34}$$

The transmission conditions (32) for two consequent subsections are then as

$$\mathbf{u}_i(l_i) = \mathbf{u}_{i+1}(0), \tag{35}$$

and the vector $\mathbf{u}_i(z_i)$ can be expressed via the initial values $\mathbf{u}_i(0)$ and the Krylov functions

$$\mathbf{u}_i(z_i) = A_i(z_i)\mathbf{u}_i(0). \tag{36}$$

Here, $A_i(z_i)$ is the matrix

$$A_i(z_i) = \begin{bmatrix} S & \frac{1}{\beta_i}T & \frac{1}{\beta_i^2D_i}U & \frac{1}{\beta_i^3D_i}V \\ \beta_iV & S & \frac{1}{\beta_iD_i}T & \frac{1}{\beta_i^2D_i}U \\ \beta_i^2D_iU & \beta_iD_iV & S & \frac{1}{\beta_i}T \\ \beta_i^3D_iT & \beta_i^2D_iU & \beta_iV & S \end{bmatrix},$$

where arguments in the Krylov functions are β_iz_i.

Based on Eqs. (36) and (35), we get the following formula:

$$\mathbf{u}_{i+1}(z_{i+1}) = A_{i+1}(z_{i+1})A_i(l_i)\mathbf{u}_i(0). \tag{37}$$

Using relations (35)–(37), solutions on each subsection can be expressed through the initial value $\mathbf{u}_1(0)$ on the first section

$$\mathbf{u}_i(z_i) = A_i(z_i)\prod_{j=i-1}^{1}A_j(l_j)\mathbf{u}_1(0). \tag{38}$$

In view of expression (38), we get the formula for displacements and forces on the right end of the beam depending on displacements and forces on the left end

$$\mathbf{u}_k(l_k) = P\mathbf{u}_i(0), \tag{39}$$

where $P = \prod_{i=k}^{1}A_i(l_i)$. The solution should be subject to the boundary conditions corresponding to either clamped or free ends of the first and last subsections. In the case of the free ends, these are

$$u_{31}(0) = u_{41}(0) = u_{3k}(l_k) = u_{4k}(l_k) = 0. \tag{40}$$

Using Eq. (39), we obtain the following equation to find the eigenfrequencies:

$$p_{31}p_{42} - p_{32}p_{41} = 0 \tag{41}$$

in which p_{ij} are elements of the matrix P. For the clamped-ends, the frequency equation (41) transforms to

$$p_{13}p_{24} - p_{14}p_{23} = 0. \tag{42}$$

Employing the normalization condition $u_{11}(0) = 1$, the initial conditions can be presented as

$$\mathbf{u}_1(0) = \{1, u_{21}(0), 0, 0\}^T, \quad u_{21}(0) = -\frac{p_{31}}{p_{32}}. \tag{43}$$

In view of the formulas (38) and (43), the eigenmodes for each subsection take the form

$$\eta_i(z_i) = b_{11}^{(i)}(z_i) - b_{12}^{(i)}(z_i)\frac{p_{31}}{p_{32}}, \quad (0 \leqslant z_i \leqslant l_i), \tag{44}$$

where $b_{pq}^{(i)}$ are elements of the matrix $B(z_i) = A_i(z_i)\prod_{j=i-1}^{1}A_j(l_j)$.

4. Numerical results and comparative analysis

4.1. BSB versus BBB systems

Henceforth, eigenfrequencies and eigenmodes of BSB and BBB systems are studied with the clamped-end conditions for the two attached beams. The nondimensional eigenfrequencies for the BSB-system are denoted ω_i, but ω_i^* are the nondimensional eigenfrequencies of the BBB-system. These three-element systems introduce a sufficient number of independent nondimensional input parameters, so that a comparative parametric analysis (by the full set of these parameters) becomes generally impossible without assuming some realistic relations between them that reduce the number of the independent parameters. Appropriate relations can be taken from the paper by Shveiko et al. (1968) who considered a spacecraft object for which the nondimensional input parameters are linked by

$$\frac{m_1}{\zeta_1} = \frac{m_2}{\zeta_2} = \frac{m}{\zeta} = 2.2; \quad \zeta = \frac{1}{75h}; \quad \nu = 0.3; \quad \frac{z_3}{R} = 20. \tag{45}$$

When adopting (45), the eigenoscillations become a function of the *nondimensional shell thickness* (proportional to $1/\zeta$), the *nondimensional shell length* (γ) and the *nondimensional shell position* (γ_1).

Fig. 2 demonstrates the three lowest eigenfrequencies of the three-element systems (BBB and the beam-type eigenoscillations of the BSB-system) versus the aforementioned three independent

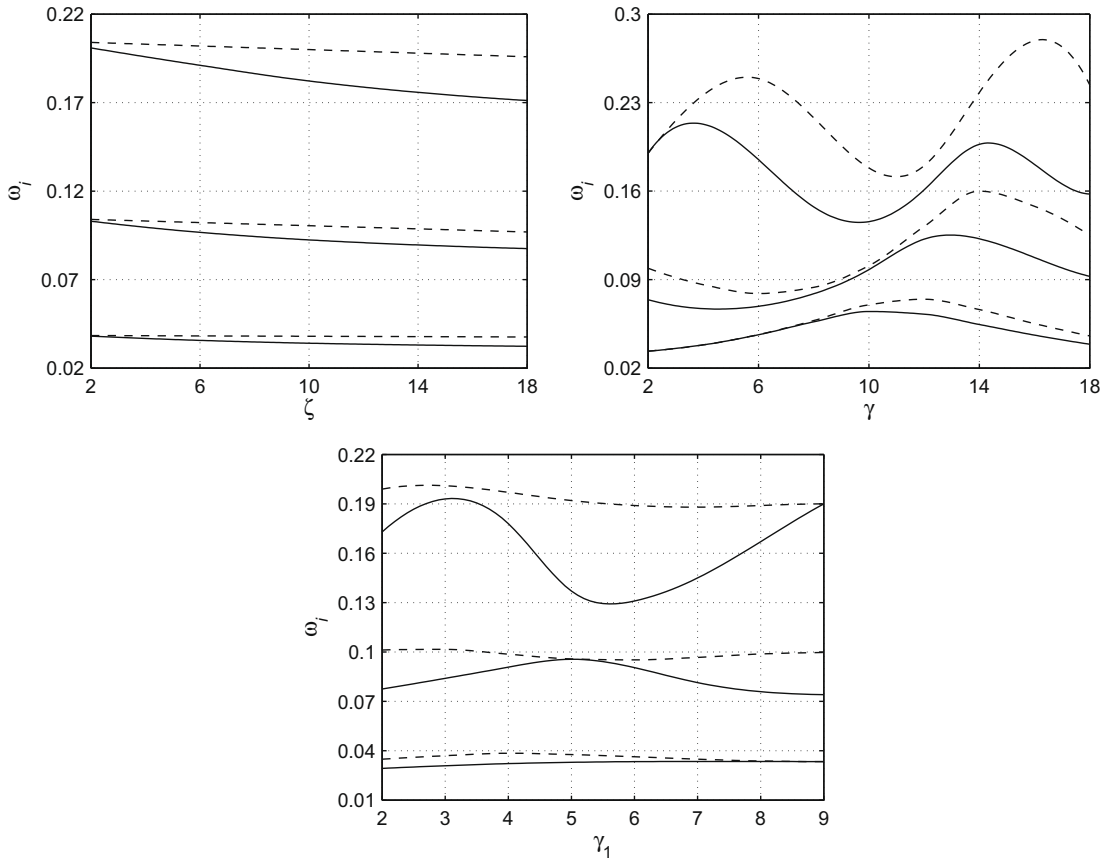

Fig. 2. The eigenfrequencies versus the nondimensional shell thickness ($\sim 1/\zeta$), the shell length (γ) and the shell position (γ_1). The remaining input nondimensional parameters are restricted to conditions (45). The clamped-end conditions are fulfilled for the beam ends; the beam-type eigenoscillations. The solid line indicates the BSB-system, the dashed line indicates the BBB-system.

input parameters ζ, γ and γ_1. The focus is on quantification of the maximum difference between the eigenfrequencies.

When comparing BSB- and BBB-eigenfrequencies versus ζ (first frame in Fig. 2), the remaining two nondimensional parameters are fixed, $\gamma = 2$ and $\gamma_1 = 4$ in this example. One can see that decreasing the shell thickness increases the drop of ω_i relative to ω_i^*. For $\zeta = 2$, the difference is about 3%, but increasing ζ to 14 causes the 10%-relative difference, namely, the larger value of ζ causes the larger drop.

Dependence of the lower eigenfrequencies on the nondimensional shell [central beam] length is presented in the second frame of Fig. 2. The remaining nondimensional parameters were chosen to provide the same total nondimensional length = 20 and equal lengths of the attached beams ($\gamma_1 = \gamma_2$); the shell thickness is restricted to $h/R = 1/900$. The graphs in this frame are quite complicated, and the eigenfrequencies drop is a non-monotonic function of γ. A reason is that a change the shell [central beam] length effects the 'total rigidity' of the composite systems of the same total length. It is impossible to formulate a rule when the drop reaches its maximum. In particular, one can see that, as long as $\gamma \leqslant 8$, the eigenfrequencies ω_1 and ω_1^* are practically the same, but the eigenfrequencies ω_3 and ω_3^* have close values for $\gamma < 4$. The minimal difference for the eigenfrequencies ω_2 and ω_2^* (about 7%) is established for $8 < \gamma < 11$. Thus, there is a difference from the first panel in Fig. 2 which means that working with a practical problem may need a dedicated numerical study on the eigenfrequencies to conclude on which from the systems is more adequate in describing the eigenoscillations. Standard design criteria are in general not applicable.

The latter conclusion is true for the last case in Fig. 2 representing dependency of the eigenfrequencies on the γ_1. In calculations, we assumed $\gamma = 2$ and $R/h = 900$.

In summary-1, our comparative numerical analysis shows that the condition $\omega_i \leqslant \omega_i^*$ is always fulfilled for the coupled vibrations of the considered three-element systems and quantifies the drop of ω_i versus three input parameters. It was shown that the difference between the eigenvalues is a non-trivial function of the nondimensional shell length and the nondimensional shell position, especially for higher eigenfrequencies. The closeness of the lower eigenfrequencies of these two different systems may require a thick and short shell with almost equal lengths of the two attached beams.

Let us now take a look at the eigenmodes. Fig. 3 illustrates the lower eigenmodes of BSB and BBB systems. For the BSB-system, the beam-type eigenmodes are modeled by $\eta_{1i}(\alpha_1)$ on $[0,z_1]$, by $w_{1i}(\alpha)$ on $[z_1,z_2]$ and by $\eta_{2i}(\alpha_2)$ on $[z_2,z_3]$. The first frame in Fig. 3 represents the case of two equal attached beams. In that case, the first and third eigenmodes of the composite systems practically coincide, but the second eigenmode differs. The second frame in Fig. 3 illustrates two lower eigenmodes for the case of non-equal lengths of the attached beams with $\gamma_1 = 2$. This 'antisymmetric' case causes reasonable difference for the lowest eigenmodes of the BSB and BBB systems; it is therefore more dangerous in modeling.

There is an expectation that the closeness of the lower eigenfrequencies of the BSB and BBB systems means that the BBB-system is generally applicable for modeling the composite constructions formed by them. However, it is wrong expectation. Even though

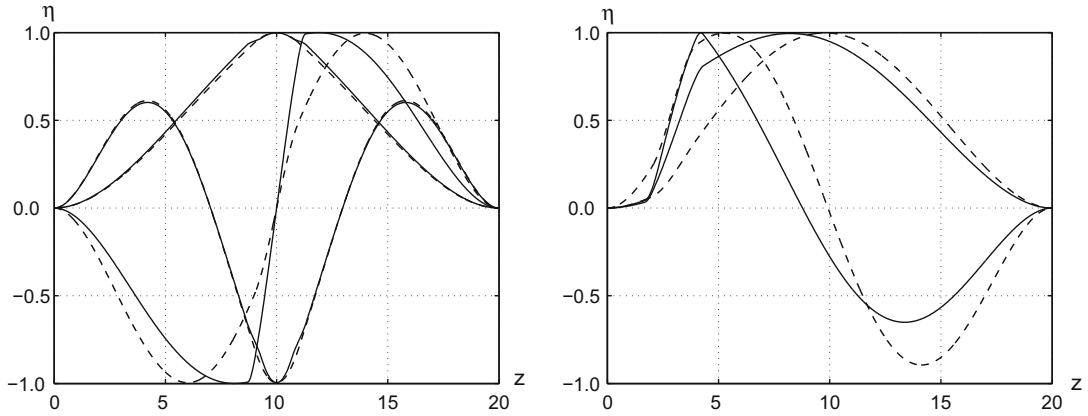

Fig. 3. The lower eigenmodes of the BSB and BBB systems. For the BSB-system, the beam-type eigenmodes are modeled by $\eta_{1i}(\alpha_1)$ on $[0,z_1]$, by $w_{1i}(\alpha)$ on $[z_1,z_2]$ and by $\eta_{2i}(\alpha_2)$ on $[z_2,z_3]$. The clamped-end conditions are satisfied for the attached beams. The input nondimensional parameters are restricted to conditions (45) providing the same nondimensional total length equal to 20. The first frame gives the three lowest eigenmodes for $\gamma = 2$, $\gamma_1 = 9$, $R/h = 900$. The second frame corresponds to $\gamma = 2$, $\gamma_1 = 2$, $R/h = 900$ and shows the two lower eigenmodes. The solid line indicates the BSB-system, the dashed line indicates the BBB-system.

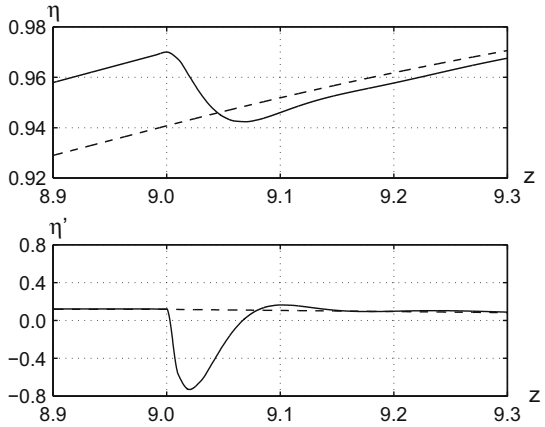

Fig. 4. Behavior of the first eigenmode and its first-order derivative in a neighborhood of the joining for $\gamma = 2$, $\gamma_1 = 9$, $R/h = 900$ (two equal attached beams). For the BSB-system, the beam-type eigenmodes are modeled by $\eta_{1i}(\alpha_1)$ on $[0,z_1]$, by $w_{1i}(\alpha)$ on $[z_1,z_2]$ and by $\eta_{2i}(\alpha_2)$ on $[z_2,z_3]$. The clamped-end conditions are satisfied for the attached beams. The input nondimensional parameters are restricted to conditions (45). The total nondimensional length equals to 20, the two attached beams are equal. The solid lines indicates BSB-system, the dashed line indicates BBB-system.

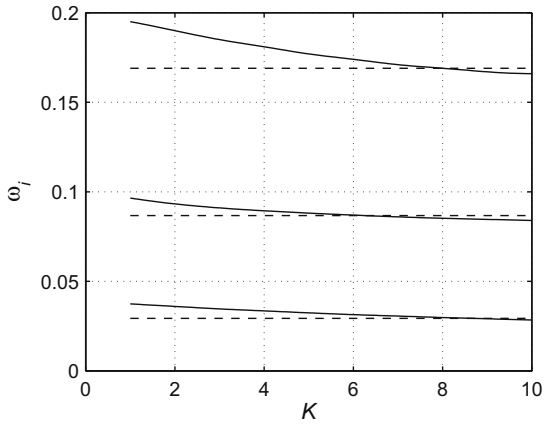

Fig. 5. Eigenfrequencies versus the corrector factor K of the bending rigidity; the linear mass does not change. The solid lines corresponds the BBB-system, the dashed line implies the BSB-system. The case of the first frame in Fig. 2 with $\zeta = 18$.

the lowest eigenmodes of BSB and BBB systems are very close to each other, as in the case of two equal attached beams in the first frame of Fig. 3, the corresponding eigenmodes may dramatically differ from each other, especially, in a neighborhood of the shell[-beam]–beam joining. The typical behavior of the first eigenmode and its first-order derivative in the neighborhood is demonstrated in Fig. 4 ($\gamma = 2$, $\gamma_1 = 9$ and $R/h = 900$). Fig. 4 shows a narrow zone in which the BSB-eigenmode changes with a high slope at the joining point. This means that analysis on applicability of the BBB-model must include comparison of the associated eigenmodes, too.

In summary-2, two non-equal attached beams lead to a sufficient difference between the lower eigenmodes of BSB and BBB systems. An exception is the case of the two equal beams attached to the shell [beam] ends, for which the lower eigenmode of these two composite systems is generally close to each other. The difference is only in a neighborhood of the shell[beam]–beam joining. The size of this neighborhood depends on how large is 'jump' in the rigidities between shell and beam at the joining point. The fact of close eigenfrequencies for the BBB and BSB systems does not mean that the eigenmodes are also close.

In accordance with our original formulation (transmission conditions), the eigenmodes and their first-order derivative are continuous at the joining. When employing the BBB-system, one can introduce a corrector-factor K for the rigidity, $(EI)^* = EI/K$ on $[z_1,z_2]$ so that the eigenfrequencies ω_i^* and ω_i coincide; the linear mass remains the same. The first three eigenfrequencies (solid lines) versus the bending rigidity are presented in Fig. 5. The figure demonstrates that the K-values, for which $\omega_i^* = \omega_i$ (intersections with the horizontal dashes lines), are different for different eigenmodes. These values are approximately equal to $K = 8$,$K = 6$ and $K = 9$ for the first, second and third mode, respectively, and can be adopted as a design criterion.

4.2. Shell–beam (SB) and shell–rigid body (SrB) systems

Similar comparative analysis is also possible for the eigenoscillations of the two-component shell–beam (SB) system, and the system consisting of a circular cylindrical shell attached to a rigid body (the SrB-system). An analysis of the SrB-system can be found in the paper by Pellicano (2007) who proposed a solution method based on the Sanders–Koiter theory as well as in the paper by Trotsenko (2006). We refer interested readers to these publications.

In the forthcoming illustrative computations, we consider the shell with the clamped-end condition, namely, (29) is satisfied;

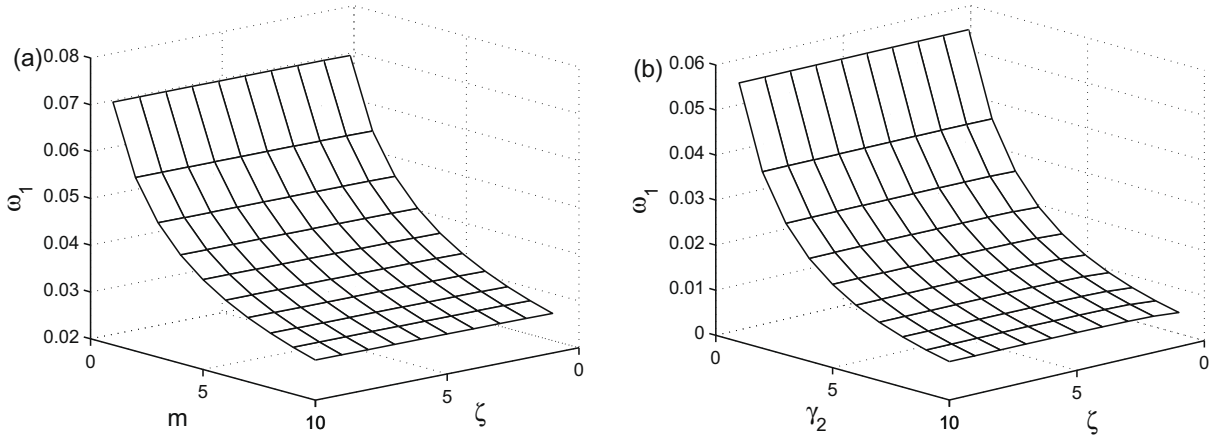

Fig. 6. The first eigenfrequency of the SB-system for different input parameters. (a) $\gamma_2 = 2$, (b) $m = 5$ with $\gamma = 4$.

the attached beam end is restricted to the free-end condition, namely, condition (30) is fulfilled at $\alpha_2 = 0$. The calculations below are done with the nondimensional values $\nu = 0.3$ and $h = 0.1$. The first frame of Fig. 6 demonstrates the first eigenfrequency of the SB-system as function of m, γ, ζ and γ_2. Within the framework of the adopted boundary conditions, effect of the nondimensional beam rigidity is of importance. Increasing ζ leads to larger eigenfrequencies, however, this affects only the third significant figure. Analogous behavior is established for higher eigenfrequencies.

The beam linear mass m and the beam length γ_2 considerably effect the eigenfrequencies. Increasing these parameters leads to a fast decrease of eigenfrequencies. One should note that a considerable increase of the beam mass and its rigidity establishes that the two lower eigenfrequencies tend to zero. Furthermore, the third eigenfrequency tends to the lowest eigenfrequency of an auxiliary shell which has two fixed ends. For instance, when we pose m and ζ equal to 10^6, the eigenfrequencies are $\omega_1 = 0.30588$, $\omega_2 = 0.57335$ and $\omega_3 = 0.76007$. These coincide with corresponding frequencies of the shell with the clamped ends and $\gamma = 4$. Trotsenko (2006) reported the same behavior for the SrB-system.

Fig. 7 illustrates effect of the beam rigidity ζ on the first three eigenmodes of the SB-system. Calculations are done with $\gamma = \gamma_2 = 4$ and $m = 5$. It shows that increasing ζ leads to considerable changes in the eigenmodes. The same is true for higher modes. Nevertheless, relatively large values of ζ lead to a fictitious beam, whose shape is close to a strain line. This allows for an assumption

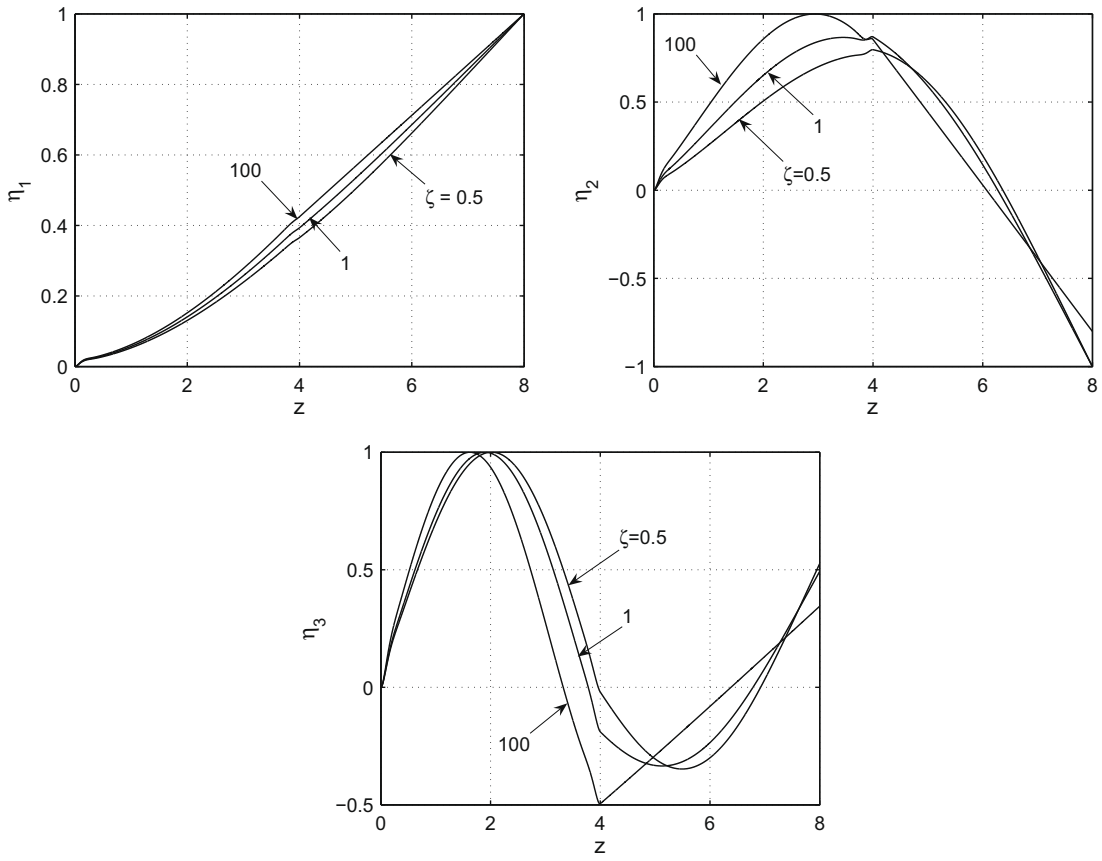

Fig. 7. The first three eigenmodes of the SB-system for different beams' rigidities ζ with $\gamma = \gamma_2 = 4$ and $m = 5$.

Table 3
The first three eigenfrequencies of the SB- (ω_i) and SrB- (ω_i^*) systems versus γ_2 for $\gamma = 10$, $m = 5$ and $\zeta = 10^6$.

γ_2	ω_1^*	ω_1	ω_2^*	ω_2	ω_3^*	ω_3
1.0	0.01541	0.01543	0.08461	0.08536	0.19950	0.20202
2.0	0.01489	0.01191	0.07937	0.07490	0.18877	0.18467
4.0	0.01384	0.00813	0.06940	0.05994	0.17039	0.15493
6.0	0.01284	0.00608	0.06138	0.04895	0.15873	0.13569
8.0	0.01191	0.00478	0.05542	0.04109	0.15171	0.12519
10.0	0.01105	0.00389	0.05106	0.03549	0.14726	0.1191

that the beam behaves as a rigid body. Obviously, varying ζ and m/ζ, one can reach a full consistence between the eigenfrequencies for the SB- and SrB-systems. However, a practical matter consists of comparing the numerical results with the same nondimensional parameters, joint for both the beams and the rigid body, namely, the linear mass m and the corresponding length γ_2. The rigidity must be large enough.

Table 3 presents the first three eigenfrequencies of the SB- (ω_i) and SrB- (ω_i^*) systems versus γ_2 with $\gamma = 10$ and $\zeta = 10^6$. It is assumed that nondimensional masses of the body and the beam are the same and equal to $m = 5$. We assumed that the rigid body has cylindrical shape of radius R and length γ_2. As long as $\gamma_2 = 1$, the eigenfrequencies obtained by using the two systems coincide with each other. However, the frequencies ω_i are slightly higher of ω_i^*. Increasing γ_2 implies decrease of the eigenfrequencies. As far as $\gamma_2 > 2$, ω_i become considerably lower of ω_i^*.

Fig. 8 illustrates effect of the shell length γ_2 on the first three eigenmodes for the SB- and SrB-systems. It shows a reasonable difference when increasing γ_2 and for higher modes.

5. Concluding remarks

In the present paper, we have proposed a new semi-analytical method for solving the problem on eigenoscillations of composite mechanical systems consisting of shell, beam, and, possibly, a rigid body. The method is less universal comparing with the Finite Element Method, but our numerical experiments (see, Section 3.1) show that it provides a fast convergence and a satisfactory accuracy with a relatively low number of coordinate functions. The method is CPU-efficient and may have clear advantages in modeling multicomponent structures.

Based on the method, a comparative quantitative analysis on the eigenfrequencies and the eigenmodes of BSB and BBB systems was conducted. Dependencies on the shell thickness, length, and position of the central object (shell or beam) were numerically studied. Summary-1 and summary-2 of Section 4.1 gain an insight into the quantitative differences. There are rather expected results. In particular, the closeness of the lower eigenfrequencies of these two different systems requires a thick and short shell with almost equal lengths of the two attached beams. However, the quantitative drop of the BSB-eigenfrequencies relative to those of the BBB-system is a non-trivial function of the input parameters responsible for the shell length and the shell position between two, possibly, not equal beams. It is difficult to predict when the drop reaches its maximum. A general recommendation is to perform *a priori* estimate of the BSB-eigenfrequencies by using a simple numerical method like the present method.

Another important fact is that, even though we deal with two symmetric (equal) attached beam which provide a consistency between the lowest beam-type eigenmode of the BSB-system and the lowest eigenmode of the BBB-system, there exist a serious differ-

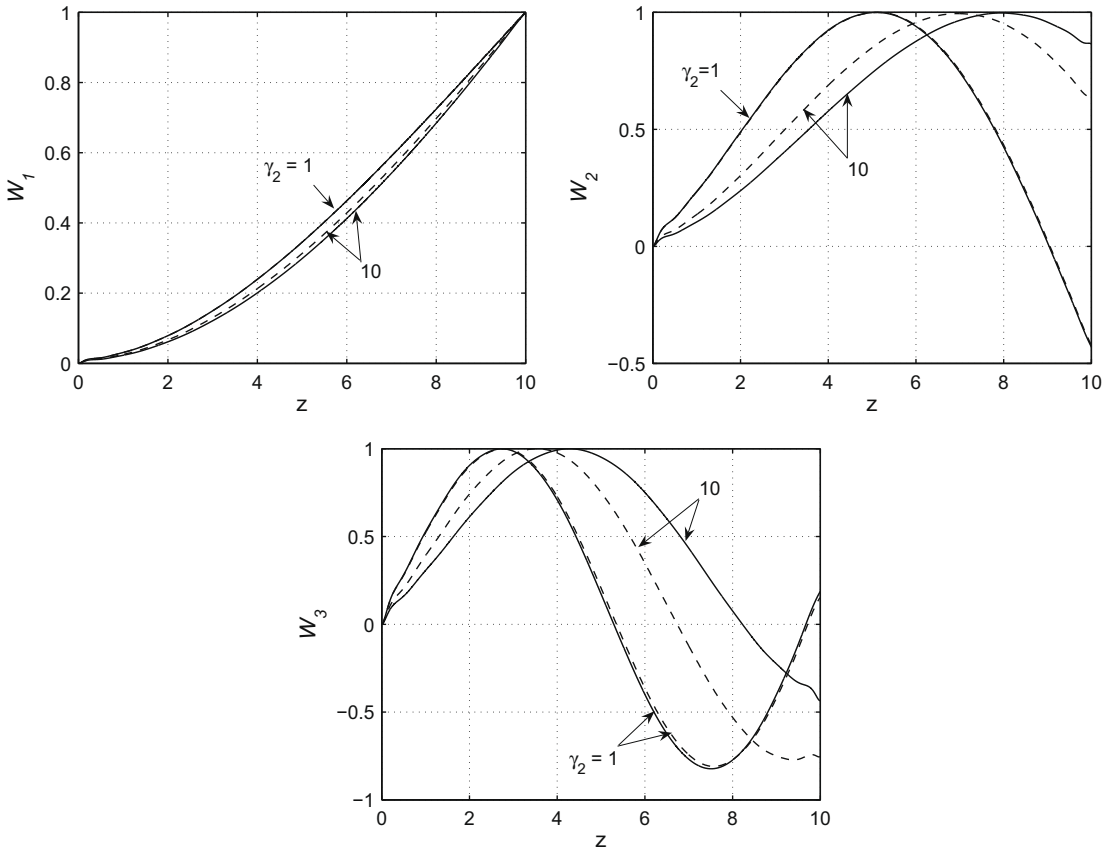

Fig. 8. The first three eigenfrequencies W_i versus γ_2 for the SB-system (solid line) and the SrB-body system (dashed line) with $\gamma = 4$, $m = 5$ and $\zeta = 10^6$.

ence between the eigenmodes in a local neighborhood of the shell–beam joining. The difference is a function of jump of the rigidities. As far as the design involves the eigenmodes, the reliable calculations should employ the BSB-model instead of the BBB-model. Finally, we cannot conclude on the closeness of the eigenmodes by employing the closeness of the eigenfunctions. Along with the aforementioned local differences at the joining, one can expect a global difference for certain cases.

When studying eigenoscillations of the SB-system, we showed that the eigenfrequencies are sensitive to varying the beam mass m and its length γ_2. Effect of the beam rigidity was found to be not so important. Comparative analysis of the eigenoscillations for the SB- and SrB-systems reflects satisfactory agreement between them for relatively short beams. In view of practical convenience, the SrB-system is much more preferable. However, ignoring the body flexibility may lead to larger theoretical eigenfrequencies. The body length is primary factor that influences the eigenfrequencies and modes.

Acknowledgements

The authors are grateful for financial support made by the DFG.

Appendix A. Dynamic equations and transmission conditions

To derive dynamic equations and transmission conditions, we can, for instance, use equivalence of the virtual work done by external forces (here, inertia forces) and variation of the potential energy due to small deviation relative to the static state

$$\delta\Pi = \delta A. \tag{A.1}$$

The potential energy of the shell can be presented within the framework of the Mushtari–Donnell–Vlasov theory (Novozhilov, 1964). Because of our simplification, contribution to the potential energy from the beams is associated with flexure in the Oxz-plane. The potential energy of the whole BSB-system is therefore

$$\begin{aligned}\Pi = {} & \frac{Eh}{2(1-\nu^2)}\int\int_\Sigma\left[\left(\frac{\partial u}{\partial z}\right)^2+\frac{1}{R^2}\left(\frac{\partial v}{\partial\varphi}+w\right)^2+\frac{2\nu}{R}\frac{\partial u}{\partial z}\left(\frac{\partial v}{\partial\varphi}+w\right)\right.\\ & \left.+\frac{1-\nu}{2}\left(\frac{1}{R}\frac{\partial u}{\partial\varphi}+\frac{\partial v}{\partial z}\right)^2\right]d\Sigma+\frac{D}{2}\int\int_\Sigma\left[\left(\frac{\partial^2 w}{\partial z^2}\right)^2+\left(\frac{1}{R^2}\frac{\partial^2 w}{\partial\varphi^2}\right)^2\right.\\ & \left.+\frac{2\nu}{R^2}\frac{\partial^2 w}{\partial z^2}\frac{\partial^2 w}{\partial\varphi^2}+2(1-\nu)\left(\frac{1}{R}\frac{\partial^2 w}{\partial z\partial\varphi}\right)^2\right]d\Sigma\\ & +\frac{1}{2}\int_0^{z_1}E_1I_1\left(\frac{\partial^2\xi_1}{\partial z^2}\right)^2dz+\frac{1}{2}\int_{z_2}^{z_3}E_2I_2\left(\frac{\partial^2\xi_2}{\partial z^2}\right)^2dz,\end{aligned} \tag{A.2}$$

where $D = Eh^3/(12(1-\nu^2))$. The first integral (over Σ) in Eq. (A.2) implies the potential energy due stretch and shear deformations of the shell. The second integral is caused by bending and torsion deformations.

Variations of the potential energy (A.2) are expressed as

$$\begin{aligned}\delta\Pi = {} & -\frac{Eh}{(1-\nu^2)}\int\int_\Sigma\{[L_{11}(u)+L_{12}(v)+L_{13}(w)]\delta u\\ & +[L_{21}(u)+L_{22}(v)+L_{23}(w)]\delta v-[L_{31}(u)+L_{32}(v)\\ & +L_{33}(w)]\delta w\}d\Sigma+\int_\Gamma\left[T_1\delta u+S\delta v+Q_1^*\delta w-M_1\frac{\partial\delta w}{\partial z}\right]\Bigg|_{z=z_1}^{z=z_2}ds\\ & +\int_0^{z_1}\frac{\partial^2}{\partial z^2}\left(E_1I_1\frac{\partial^2\xi_1}{\partial z^2}\right)\delta\xi_1\,dz+\left(M^{(1)}\frac{\partial\delta\xi_1}{\partial z}-Q^{(1)}\delta\xi_1\right)\Bigg|_{z=0}^{z=z_1}\\ & +\int_{z_2}^{z_3}\frac{\partial^2}{\partial z^2}\left(E_2I_2\frac{\partial^2\xi_2}{\partial z^2}\right)\delta\xi_2\,dz+\left(M^{(2)}\frac{\partial\delta\xi_2}{\partial z}-Q^{(2)}\delta\xi_2\right)\Bigg|_{z=z_2}^{z=z_3}.\end{aligned} \tag{A.3}$$

Here, we adopted notations (10) and (12).

The virtual work caused by the inertia forces and virtual displacements δu, δv, δw and $\delta\xi_k$ can be presented as

$$\begin{aligned}\delta A = {} & -\rho h\int\int_\Sigma\left(\frac{\partial^2 u}{\partial t^2}\delta u+\frac{\partial^2 v}{\partial t^2}\delta v+\frac{\partial^2 w}{\partial t^2}\delta w\right)d\Sigma\\ & -\int_0^{z_1}m_1\frac{\partial^2\xi_1}{\partial t^2}\delta\xi_1\,dz-\int_{z_2}^{z_3}m_2\frac{\partial^2\xi_2}{\partial t^2}\delta\xi_2\,dz.\end{aligned} \tag{A.4}$$

Variations δu, δv, δw and $\delta\xi_k$ depend on contours formed by the contact points of shell and beams. The functions δu, δv, δw and $\delta\xi_k$ are subject to Eqs. (5) and (6). Accounting for this fact, substitution of (A.3) and (A.4) into Eq. (A.1) gives the partial differential equations (9), boundary conditions (7) or (8) on the beams ends and the dynamic transmission conditions (11) on the two shell ends.

Appendix B. Expressions for elements of matrices *A* and *B*

The following integrals are introduced:

$$\Phi_1(f,h)=\int_0^\gamma[\Psi_{11}(f,f)-2\Psi_{13}(h,f)+\Psi_{33}(h,h)]d\alpha;$$

$$\Phi_2(f,h)=\int_0^\gamma[\Psi_{22}(f,f)-2\Psi_{23}(h,f)+\Psi_{33}(h,h)]d\alpha;$$

$$\Phi_3(f,g,h)=\int_0^\gamma[\Psi_{12}(f,f)-\Psi_{13}(g,f)-\Psi_{23}(h,f)+\Psi_{33}(h,g)]d\alpha;$$

$$F_1=\int_0^\gamma[-\Psi_{11}(f_2,f_1)+\Psi_{13}(h_2,f_1)+\Psi_{13}(h_1,f_2)-\Psi_{33}(h_2,h_1)]d\alpha;$$

$$F_2=\int_0^\gamma[\Psi_{12}(f_2,f_1)-\Psi_{13}(g_2,f_1)-\Psi_{23}(h_1,f_2)+\Psi_{33}(g_2,h_1)]d\alpha;$$

$$F_3=\int_0^\gamma[-\Psi_{12}(f_1,f_2)+\Psi_{13}(g_1,f_2)+\Psi_{23}(h_2,f_1)-\Psi_{33}(h_2,g_1)]d\alpha;$$

$$F_4=\int_0^\gamma[\Psi_{22}(f_2,f_1)-\Psi_{23}(g_2,f_1)-\Psi_{23}(g_1,f_2)+\Psi_{33}(g_2,g_1)]d\alpha;$$

$$\alpha_{11}(i)=\int_0^\gamma[\Psi_{13}(h_1,U_i)-\Psi_{11}(f_1,U_i)]d\alpha;$$

$$\alpha_{12}(i)=\int_0^\gamma[\Psi_{13}(g_1,U_i)-\Psi_{12}(f_1,U_i)]d\alpha;$$

$$\alpha_{13}(i)=\int_0^\gamma[\Psi_{13}(h_2,U_i)-\Psi_{11}(f_2,U_i)]d\alpha;$$

$$\alpha_{14}(i)=\int_0^\gamma[\Psi_{13}(g_2,U_i)-\Psi_{12}(f_2,U_i)]d\alpha;$$

$$\alpha_{21}(i)=\int_0^\gamma[\Psi_{23}(h_1,V_i)-\Psi_{12}(V_i,f_1)]d\alpha;$$

$$\alpha_{22}(i)=\int_0^\gamma[\Psi_{23}(g_1,V_i)-\Psi_{22}(f_1,V_i)]d\alpha;$$

$$\alpha_{23}(i)=\int_0^\gamma[\Psi_{23}(h_2,V_i)-\Psi_{12}(V_i,f_2)]d\alpha;$$

$$\alpha_{24}(i)=\int_0^\gamma[\Psi_{23}(g_2,V_i)-\Psi_{22}(f_2,V_i)]d\alpha;$$

$$\alpha_{31}(i)=\int_0^\gamma[\Psi_{33}(h_1,W_i)-\Psi_{13}(W_i,f_1)]d\alpha;$$

$$\alpha_{32}(i)=\int_0^\gamma[\Psi_{33}(g_1,W_i)-\Psi_{23}(W_i,f_1)]d\alpha;$$

$$\alpha_{33}(i)=\int_0^\gamma[\Psi_{33}(h_2,W_i)-\Psi_{13}(W_i,f_2)]d\alpha;$$

$$\alpha_{34}(i)=\int_0^\gamma[\Psi_{33}(g_2,W_i)-\Psi_{23}(W_i,f_2)]d\alpha.$$

The beams functions $U(\beta_k\alpha_k)$, $V(\beta_k\alpha_k)$ and their first derivatives at $\alpha_k=\gamma_k$ ($k=1,2$) are denoted as

$$u_{0k} = U(\beta_k\gamma_k); \quad v_{0k} = V(\beta_k\gamma_k); \quad u'_{0k} = \left.\frac{dU(\beta_k\alpha_k)}{d\alpha_k}\right|_{\alpha_k=\gamma_k},$$

$$v'_{0k} = \left.\frac{dV(\beta_k\alpha_k)}{d\alpha_k}\right|_{\alpha_k=\gamma_k}; \quad (u_{0k}v_{0k})' = \left.\frac{d}{d\alpha_k}[U(\beta_k\alpha_k)V(\beta_k\alpha_k)]\right|_{\alpha_k=\gamma_k}.$$

Within the introduced notations, the over-diagonal elements of A can be presented as

$$a_{i,j} = \int_0^\gamma \Psi_{11}(U_j,U_i)\,d\alpha; \;\; a_{i,j+N} = \int_0^\gamma \Psi_{12}(V_j,U_i)\,d\alpha;$$
$$a_{i,j+2N} = \int_0^\gamma \Psi_{13}(W_j,U_i)\,d\alpha; \;\; a_{i+N,j+N} = \int_0^\gamma \Psi_{22}(V_j,V_i)\,d\alpha;$$
$$a_{i+N,j+2N} = \int_0^\gamma \Psi_{23}(W_j,V_i)\,d\alpha; \;\; a_{i+2N,j+2N} = \int_0^\gamma \Psi_{33}(W_j,W_i)\,d\alpha;$$
$$a_{i,N_1} = u'_{01}\alpha_{11}(i) + u_{01}\alpha_{12}(i); \;\; a_{i,N_2} = v'_{01}\alpha_{11}(i) + v_{01}\alpha_{12}(i);$$
$$a_{i,N_3} = -u'_{02}\alpha_{13}(i) + u_{02}\alpha_{14}(i); \;\; a_{i,N_4} = -v'_{02}\alpha_{13}(i) + v_{02}\alpha_{14}(i);$$
$$a_{i+N,N_1} = u'_{01}\alpha_{21}(i) + u_{01}\alpha_{22}(i); \;\; a_{i+N,N_2} = v'_{01}\alpha_{21}(i) + v_{01}\alpha_{22}(i);$$
$$a_{i+N,N_3} = -u'_{02}\alpha_{23}(i) + u_{02}\alpha_{24}(i); \;\; a_{i+N,N_4} = -v'_{02}\alpha_{23}(i) + v_{02}\alpha_{24}(i);$$
$$a_{i+2N,N_1} = u'_{01}\alpha_{31}(i) + u_{01}\alpha_{32}(i); \;\; a_{i+2N,N_2} = v'_{01}\alpha_{31}(i) + v_{01}\alpha_{32}(i);$$
$$a_{i+2N,N_3} = -u'_{02}\alpha_{33}(i) + u_{02}\alpha_{34}(i); \;\; a_{i+2N,N_4} = -v'_{02}\alpha_{33}(i) + v_{02}\alpha_{34}(i);$$
$$a_{N_1,N_1} = C^{(1)}_{11} + (u'_{01})^2\Phi_1(f_1,h_1) + 2u_{01}u'_{01}\Phi_3(f_1,g_1,h_1) + (u_{01})^2\Phi_2(f_1,g_1);$$
$$a_{N_1,N_2} = C^{(1)}_{12} + u'_{01}v'_{01}\Phi_1(f_1,h_1) + (u_{01}v_{01})'\Phi_3(f_1,g_1,h_1) + u_{01}v_{01}\Phi_2(f_1,g_1);$$
$$a_{N_1,N_3} = u'_{01}u'_{02}F_1 + u_{02}u'_{01}F_2 + u_{01}u'_{02}F_3 + u_{01}u_{02}F_4;$$
$$a_{N_1,N_4} = u'_{01}v'_{02}F_1 + v_{02}u'_{01}F_2 + u_{01}v'_{02}F_3 + u_{01}v_{02}F_4;$$
$$a_{N_2,N_2} = C^{(1)}_{22} + (v'_{01})^2\Phi_1(f_1,h_1) + 2v_{01}v'_{01}\Phi_3(f_1,g_1,h_1) + (v_{01})^2\Phi_2(f_1,g_1);$$
$$a_{N_2,N_3} = v'_{01}u'_{02}F_1 + u_{02}v'_{01}F_2 + v_{01}u'_{02}F_3 + v_{01}u_{02}F_4;$$
$$a_{N_2,N_4} = v'_{01}v'_{02}F_1 + v_{02}v'_{01}F_2 + v_{01}v'_{02}F_3 + v_{01}v_{02}F_4;$$
$$a_{N_3,N_3} = C^{(2)}_{11} + (u'_{02})^2\Phi_1(f_2,h_2) - 2u_{02}u'_{02}\Phi_3(f_2,g_2,h_2) + (u_{02})^2\Phi_2(f_2,g_2);$$
$$a_{N_3,N_4} = C^{(2)}_{12} + u'_{02}v'_{02}\Phi_1(f_2,h_2) - (u_{02}v_{02})'\Phi_3(f_2,g_2,h_2) + u_{02}v_{02}\Phi_2(f_2,g_2);$$
$$a_{N_4,N_4} = C^{(2)}_{22} + (v'_{02})^2\Phi_1(f_2,h_2) - 2v_{02}v'_{02}\Phi_3(f_2,g_2,h_2) + (v_{02})^2\Phi_2(f_2,g_2),$$

where

$$C^{(k)}_{11} = (1-\nu^2)\zeta_k\beta_k^3(ST - VU)_{\alpha_k=\gamma_k};$$
$$C^{(k)}_{12} = (1-\nu^2)\zeta_k\beta_k^3(T^2 - SU)_{\alpha_k=\gamma_k};$$

$$C^{(k)}_{22} = (1-\nu^2)\zeta_k\beta_k^3(TU - SV)_{\alpha_k=\gamma_k}; \quad k = 1,2;$$
$$N_i = 3N + i, \quad i = 1,\ldots,4.$$

Here, S, T, U and V are the Krylov functions. Expressions for U and V are given above, S and T take the following form:

$$S(\beta\alpha) = \frac{1}{2}(\cosh\beta\alpha + \cos\beta\alpha); \quad T(\beta\alpha) = \frac{1}{2}(\sinh\beta\alpha + \sin\beta\alpha).$$

Let us introduce the following integrals:

$$(f,g) = \int_0^\gamma fg\,d\alpha; \quad E(f,g) = \int_0^\gamma (f^2+g^2)\,d\alpha;$$
$$FH = \int_0^\gamma (f_1f_2 + h_1h_2)\,d\alpha; \quad FG = \int_0^\gamma (f_1f_2 + g_1g_2)\,d\alpha.$$

The corresponding elements of the matrix B can then be presented as follows:

$$b_{i,j} = (U_j,U_i); \quad b_{i,j+N} = 0; \quad b_{i,j+2N} = 0; \quad b_{i,N_1} = -u'_{01}(f_1,U_i);$$
$$b_{i,N_2} = -v'_{01}(f_1,U_i); \quad b_{i,N_3} = u'_{02}(f_2,U_i); \quad b_{i,N_4} = v'_{02}(f_2,U_i);$$
$$b_{i+N,j+N} = (V_j,V_i); \quad b_{i+N,j+2N} = 0; \quad b_{i+N,N_1} = -u_{01}(f_1,V_i);$$
$$b_{i+N,N_2} = -v_{01}(f_1,V_i); \quad b_{i+N,N_3} = -u_{02}(f_2,V_i);$$
$$b_{i+N,N_4} = -v_{02}(f_2,V_i);$$
$$b_{i+2N,j+2N} = (W_j,W_i); \quad b_{i+2N,N_1} = u_{01}(g_1,W_i) + u'_{01}(h_1,W_i);$$
$$b_{i+2N,N_2} = v_{01}(g_1,W_i) + v'_{01}(h_1,W_i);$$
$$b_{i+2N,N_3} = u_{02}(g_2,W_i) - u'_{02}(h_2,W_i);$$
$$b_{i+2N,N_4} = v_{02}(g_2,W_i) - v'_{02}(h_2,W_i);$$
$$b_{N_1,N_1} = (u'_{01})^2E(f_1,h_1) + 2u_{01}u'_{01}(g_1,h_1) + (u_{01})^2E(f_1,g_1);$$
$$b_{N_1,N_2} = u'_{01}v'_{01}E(f_1,h_1) + u_{01}v_{01}E(f_1,g_1) + (u_{01}v_{01})'(g_1,h_1);$$
$$b_{N_1,N_3} = -u'_{01}u'_{02}FH + u_{01}u_{02}FG - u_{01}u'_{02}(g_1,h_2) + u_{02}u'_{01}(g_2,h_1);$$
$$b_{N_1,N_4} = -u'_{01}v'_{02}FH + u_{01}v_{02}FG - u_{01}v'_{02}(g_1,h_2) + v_{02}u'_{01}(g_2,h_1);$$
$$b_{N_2,N_2} = (v'_{01})^2E(f_1,h_1) + 2v_{01}v'_{01}(g_1,h_1) + (v_{01})^2E(f_1,g_1);$$
$$b_{N_2,N_3} = -v'_{01}u'_{02}FH + v_{01}u_{02}FG - v_{01}u'_{02}(g_1,h_2) + u_{02}v'_{01}(g_2,h_1);$$
$$b_{N_2,N_4} = -v'_{01}v'_{02}FH + v_{01}v_{02}FG - v_{01}v'_{02}(g_1,h_2) + v_{02}v'_{01}(g_2,h_1);$$
$$b_{N_3,N_3} = (u'_{02})^2E(f_2,h_2) - 2u_{02}u'_{02}(g_2,h_2) + (u_{02})^2E(f_2,g_2);$$
$$b_{N_3,N_4} = u'_{02}v'_{02}E(f_2,h_2) + u_{02}v_{02}E(f_2,g_2) - (u_{02}v_{02})'(g_2,h_2);$$
$$b_{N_4,N_4} = (v'_{02})^2E(f_2,h_2) - 2v_{02}v'_{02}(g_2,h_2) + (v_{02})^2E(f_2,g_2).$$

References

Breslavsky, V.E., 1973. Investigation of vibrations of thin shells bound to a loading material. In: Proceedings of the VIII All-Union Conference on the Theory of Shells and Plates, Leningrad, May 21–28, 1973, Nauka, Moscow, pp. 271–276 (in Russian).

Breslavsky, V.E., 1981. Longitudinal vibrations of a cylindrical shell bound to elasto-viscous filler and lumped masses. Problems of Machinery (Problemy Mashinostroeniya) 14, 27–32 (in Russian).

Bukharinov, G.N., 1974. Oscillations of two bodies joined by a circular cylindrical shell. In: Studies on Elasticity and Plasticity (Issledovaniya po Uprugosti i Plastichnosti), Leningrad, Leningrad University, No. 2, pp. 74–80 (in Russian).

Drake, K.R., 1999. The effect of internal pipes on the fundamental frequency of liquid sloshing in a circular tank. Applied Ocean Research 21 (3), 133–143.

Dutta, S., Mandal, A., Chandra Dutta, S.C., 2004. Soil–structure interaction in dynamic behaviour of elevated tanks with alternate frame staging configurations. Journal of Sound and Vibration 277 (4–5), 825–853.

Faltinsen, O.M., Timokha, A.N., 2009. Sloshing. Cambridge University Press, Cambridge.

Forsberg, K., 1966. Axisymmetric and beam-type vibrations of thin cylindrical shells. Paper 66-447, AIAA, Fourth Aerospace Sci. Mtg., Los Angeles, California, June 27–29.

Gibson, R.F., Ayorinde, E.O., Wen, Y.-F., 2007. Vibrations of carbon nanotubes and their composities: a rewiev. Composites Science and Technology 67, 1–28.

Harik, V.M., Gates, T.S., Nemeth, M.P., 2002. Applicability of the continuum-shell theories to the mechanics of carbon nanotubes. NASA/CR-2002-211460 ICASE Report No. 2002-7.

Kiefling, L.A., Leadbetter, S.A., 1971. Vibration studies of dynamic scale model of space shuttle. Langley Research Center. In: NASA Space Shuttle Technological Conference, vol. 3, April 1971, pp. 1–25.

Krylov, A.I., 1936. Vibration of Ships. Leningrad (in Russian).

Legoas, S.B., Coluci, V.R., Braga, S.F., Coura, P.Z., Dantas, S.O., 2004. Gigahertz nanomechanical oscillators based on carbon nanotubes. Nanotechnology 15, S184–S189.

Leissa, A.W., 1993. Vibration of Shells. Acoustical Society of America, New York.

Livaoglu, R., Doganguen, A., 2006. Simplified seismic analysis procedures for elevated tanks considering fluid–structure–soil interaction. Journal of Fluids and Structures 22 (3), 421–439.

Novozhilov, V.V., 1964. Thin shell theory. second augmented and revised edition, translated from the second Russian edition by P.G. Lowe, edited by J.R.M. Radok, P. Noordhoff Ltd., Groningen, 1964, The Netherlands.

Pellicano, F., 2007. Vibrations of circular cylindrical shells: theory and experiments. Journal of Sound and Vibration 300 (1), 154–170.

Rotter, J.M., 1998. Shell structures: the new European standard and current research needs. Thin-Walled Structures 31 (1–3), 3–23.

Sharma, C.B., Johns, D.J., 1966. The structural design of shelf supporting steel chimneys. Deducted from B.S. 4076, Technol. Rept.

Sharma, C.B., Johns, D.J., 1968. Vibration studies of a ring stiffned circular cylindrical shell. Journal of Sound and Vibration 8 (1), 147–155.

Sharma, C.B., Johns, D.J., 1970. Vibration characteristics of a clamped-free and clamped ring stiffened cylindrical shell. Technol. Report TT7001, Loughborough University.

Sharma, C.B., Johns, D.J., 1971. Vibration characteristics of a clamped-free and clamped-ring-stiffened circular cylindrical shell. Journal of Sound and Vibration 14 (4), 459–467.

Shveiko, Yu.Yu., Brusilovskii, A.D., Melnikova, L.M., 1968. Transverse vibration in beams connected with a cylindrical shell. Soviet Applied Mechanics 4 (8), 28–34.

Trotsenko, Yu.V., 2002. Free oscillations of a cylindrical shell coupling elastic beams. Acoustic Bulletin 5 (2), 54–72 (in Russian).

Trotsenko, Yu.V., 2006. Frequencies and modes of vibration of a cylindrical shell with attached rigid body. Journal of Sound and Vibration 292 (8), 535–551.
Trotsenko, V.A., Kladinoga, V.S., 1994. Non-axisymmetric vibrations of a prestressed shell of revolution with an attached rigid disk. Soviet Applied Mechanics 30, 17–24.
Wu, D.H., Chien, W.T., Chen, C.S., Chen, H.H., 2006. Resonant frequency analysis of fixed-free single-walled carbon nanotube-based mass sensor. Sensors and Actuators A 126, 117–121.